DRAG FORCES ON BAFFLE BLOCKS IN A STILLING BASIN (PERGAU POND MODEL IN UTP LABORATORY)

By

Anis Sabrina bt Azahari

FINAL PROJECT REPORT

Submitted to the Civil Engineering Programme
in Partial Fulfillment of the Requirements
for the Degree
Bachelor of Engineering (Hons)
(Civil Engineering)

Universiti Teknologi Petronas
Bandar Seri Iskandar
31750 Tronoh
Perak Darul Ridzuan

© Copyright 2007
by
Anis Sabrina bt Azahari, 2007

CERTIFICATION OF APPROVAL

DRAG FORCES ON BAFFLE BLOCKS IN A STILLING BASIN (PERGAU POND MODEL IN UTP LABORATORY)

By

Anis Sabrina bt Azahari

A project dissertation submitted to the
Civil Engineering Programme
Universiti Teknologi PETRONAS
in partial fulfillment of the requirement for the
BACHELOR OF ENGINEERING (Hons)
(CIVIL ENGINEERING)

Approved:

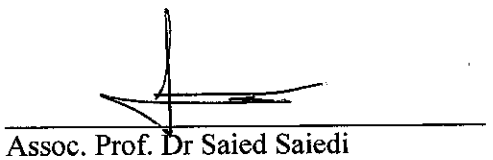

Assoc. Prof. Dr Saied Saiedi
Project Supervisor

UNIVERSITI TEKNOLOGI PETRONAS

TRONOH, PERAK

June 2007

CERTIFICATION OF ORIGINALITY

This is to certify that I am responsible for the work submitted in this project, that the original work is my own except as specified in the references and acknowledgements, and that the original work contained herein have not been undertaken or done by unspecified sources or persons.

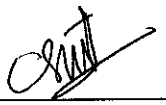

ANIS SABRINA BT AZAHARI

ABSTRACT

Baffle blocks is one type of energy dissipater functioning to dissipate excess kinetic energy possessed by flowing of water. It is also used to protect downstream area by reducing the velocity of flow to the acceptable limits. Pergau Pond Model was constructed in UTP Laboratory for investigation of Pergau Regulating Pond failure. Objective of this work is to conduct a series of laboratory tests to provide for evaluation of the existing empirical relations and possibly come up with new guides for the magnitude and behavior of the forces on the baffle blocks in a stilling basin of Pergau Pond Model in UTP Laboratory. The work is done by analyze the effect of different shape, size and discharges to the resulting drag forces. The results obtained shows that higher the frontal area, A, and height of block, higher the drag forces. The standard USBR block type provide an optimum drag force compared to sloped trapezoidal shape. It is also proved that higher discharge and velocity value resulting in higher forces. Drag force coefficient is also analyzed and studied from previous investigations. Equipment and measurement error have been found during the lab experimental procedure which affecting the experiment results. Besides, limited equipment available eliminate the better methods could be implemented while avoiding satisfied quantity of data obtained. The basic factors influencing the drag force performance has been studied and understood while the knowledge of drag forces on baffle blocks behavior is acquired.

ACKNOWLEDGEMENTS

First of all, the deepest gratitude to Allah S.W.T. for his blessing and mercy, I managed to complete this Final Year Project as a requirement of completing a Bachelors of Engineering (Hons) in Civil Engineering.

I would like to give a special thanks to my project supervisor, Assoc Prof. Dr Saied Saiedi for his support, knowledge and guidance for the one year which this project had been conducted.

Not forgotten, to all my colleagues and technicians of Civil Engineering Department for their help and encouragement. To my family as they have been given all the necessary support from the beginning.

Thank you to all parties who participate directly or indirectly in completing this work. All your contributions are highly appreciated.

Anis Sabrina bt. Azahari

TABLE OF CONTENTS

LIST OF FIGURES

LIST OF TABLES

CHAPTER 1

INTRODUCTION

1.1. Background of Study

The Regulating Pond of Pergau Hydropower Station, located 125 km from Kota Bharu, the capital of the state of Kelantan in Malaysia has experienced the failure where that part of HDPE Liner was surprisingly seen to be floating on the surface. This was indication of the damage to the pond floor through bed erosion and Liner rupture downstream of the apron. The owner, Tenaga Nasional Berhad (TNB) was appointed Universiti Teknologi PETRONAS (UTP) to do a comprehensive investigation into the causes of the damages and design of the rehabilitation works. Thus, the Pergau Pond Model was constructed to do a core investigation of the damages. In this case, baffle blocks as well as bed floor of the pond are the important parameters that were contributed to the failure. Therefore, the shapes, size and also the arrangement of the baffle blocks as an energy dissipater are the main factors affecting the bed floor condition.

1.2. Problem Statement

Since the baffle block structures are the important component of dissipating total energy to the pond, which the energy can cause a damage to the pond floor, it is important to analyze the factors affecting the total drag forces exerted by the flow since the available baffle blocks of Pergau Pond seems cannot give an optimum long-life of the entire structure. Various shape and sizes, and other factors influenced need to be studied to come out with a better block design in the future. Magnitude and behavior of the forces in a Pergau Pond stilling basin need to be investigated to improve the design control of the pond.

1.3. Objective and Scope of Study

The project objectives is to conduct a series of laboratory tests to provide for evaluation of the existing empirical relations and possibly come up with new guides for the magnitude and behavior of the forces on the baffle blocks in a stilling basin of Pergau Pond Model in UTP Laboratory.

1.3.1. Project Requirement

i. To conduct a study on behavior of the forces on a baffle blocks in a stilling basin in a Pergau Pond Model in UTP Laboratory.
ii. Getting familiar with the energy dissipation, baffle blocks and hydrodynamic forces by reading and do a data collection from internet, library and correspondence.
iii. To get familiar with the condition and equipments available in Pergau Pond Model in UTP Laboratory.
iv. To design the baffle blocks with different shapes, sizes and arrangement.
v. To do lab tests in UTP Laboratory.
vi. To collect the comparison and analyze the data obtained and come up with new guides for magnitude and behavior of the forces.

CHAPTER 2

LITERATURE REVIEW AND THEORY

2.1. Introduction to Baffle Block Structure

A baffle blocks is one of the energy dissipater which are important components of the stilling basins designed for energy dissipation of the flow released through spillway, chutes and hydropower tunnels. It is also a device used to protect downstream area by reducing the velocity of flow to the acceptable limits. When water is released over the hydropower tunnels, the potential energy is converted into kinetic energy in the stilling basin. This energy must be dissipated in order to prevent the possibility of sever scouring of downstream riverbed and the undermining of foundation which may cause failure of dam or spillway. The efficiency of the stilling basin is largely depends on the résistance offered by the baffle piers, secured in position against the drag force exerted by the flow. This is influenced by the factors such as shape, velocity entering the basin, the distance of the upstream face of the baffle from the toe of the jump, Froude number of the flow, and tail water depth. Followings are several type of baffle blocks shapes;

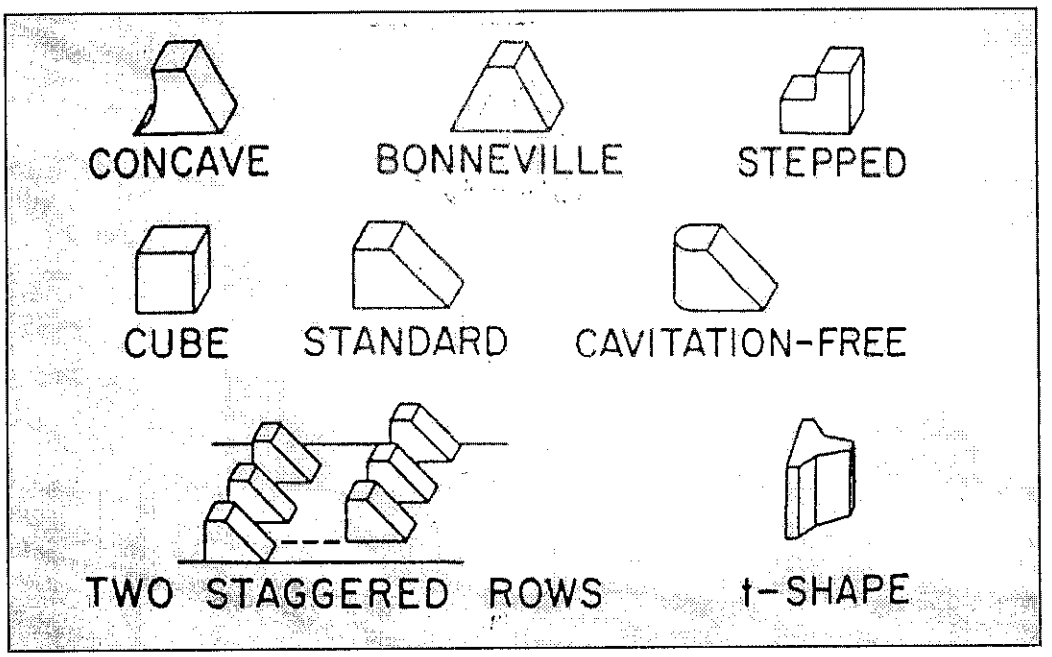

Figure 2.1: Typical Baffle Block Shapes

2.2. Drag Forces on Baffle Blocks

The drag force is the net force exerted by a fluid on a body in the direction of flow due to the combined effects of wall shear and pressure force. The drag forces depend on the density, ρ of the fluid, the upstream velocity V, and the size, shape, and orientation of the body. When water is flowing onto the baffle block, kinetic energy will be converted into the pressure force or drag force which can be computed by following equation;

$$F_D = C_D \frac{\rho V^2 A}{2}$$

Where

A = Frontal area (the area projected on a plane normal to the direction of flow), m^2

V= Velocity of moving fluid, m/s

ρ= Mass density of fluid, 1000kg/lit

C_D= Drag Coefficient

Drag coefficient is a dimensionless numbers that represent the drag characteristics of the body. These numbers obtained by modification of drag force equation which defined as;

$$C_D = \frac{2F_D}{\rho V^2 A}$$

2.3. Previous Investigations of Drag Force on Baffle Blocks

Herleman (1963) and other investigators, Robert (1956) and James (1953), were the first to actually measure forces in blocks in a jump. They found that for a given geometry, the drag force is increased as X_B decreased. The force ratio, F_B / F_2, was employed in the dimensionless plots and increased with increasing Froude number for given geometry and location. Force measurement made at the St. Anthony Falls Hydraulic Laboratory (1968) indicated the standard and T-Shape blocks produced twice as much as drag as the cavitations- free and Bonneville shapes.

Basco and Adam (1970) were employed an experimental technique to determine the drag forces by direct measurement. Instead of classical drag coefficient, the ratio of drag force on the baffle blocks to free jump hydrostatic tail water force for the same inlet Froude number, proved to be the most indicative of the effectiveness of baffle blocks in the forced jump. Followings are the sketch of basic layout of baffle blocks in flume in an experimental procedure.

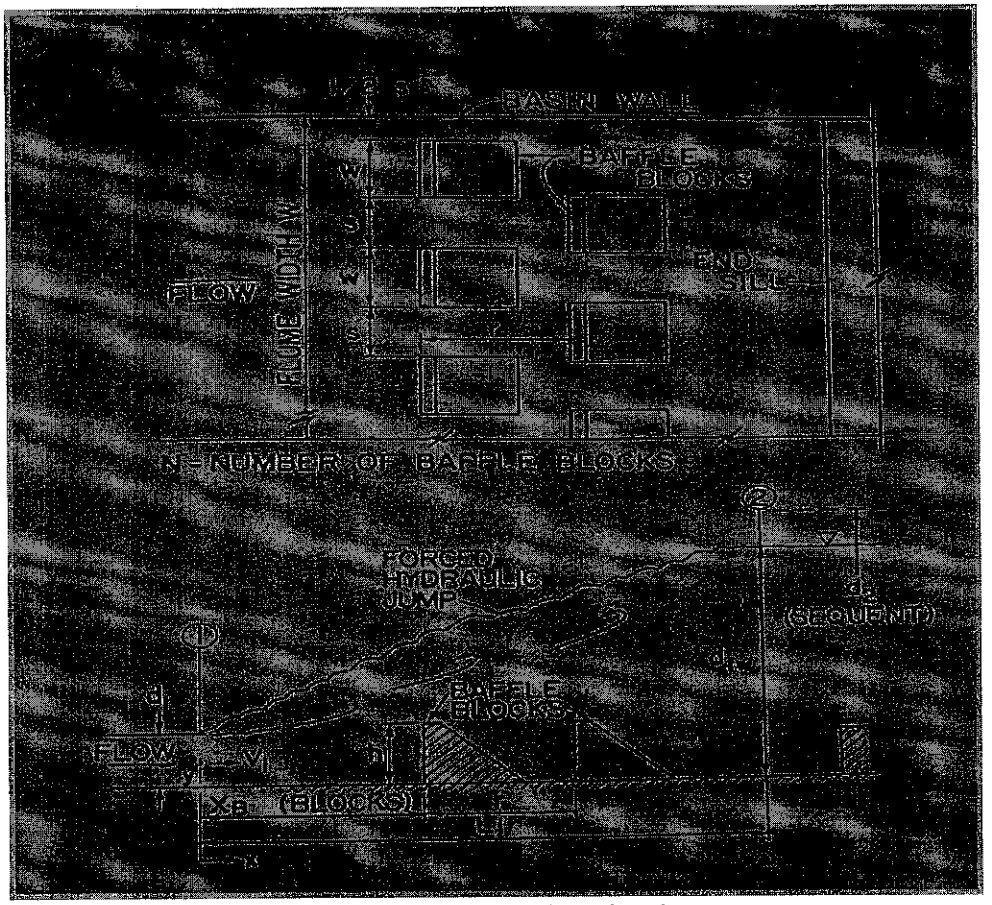

Figure 2.2: Definition Sketch

Figure 2.2 above shows the cross sectional of standard shape Baffle blocks arrangement in flume of the drag forces analysis purposes. They use of the control volume technique and application of the steady flow, linear momentum equation with the usual assumption yields

$$\frac{\gamma d_1^2}{2} - \frac{\gamma d^2{}_{tw}}{2} - \frac{F_B}{W} = \rho V_{tw}^2 d_{tw} - \rho V_1^2 d_1$$

Where F_B = the total drag force on the baffle blocks; W= the channel width; γ= the unit weight of the liquid; and ρ = the mass density of the liquid.

The momentum equation, when combined with the continuity principle, degenerates into the well- known Belanger equation:

$$\frac{d_2}{d_1} = \frac{1}{2}\left(\sqrt{1+8F_1^2} - 1\right)$$

For the free jump with no blocks, the inlet Froude number F_1 is defined as

$$F_1 = \frac{V_1}{\sqrt{gd_1}}$$

A dimensionless drag coefficient C_D, is commonly used to relate the drag force to the size, speed, and physical properties of the system. It is defined as

$$C_D = \frac{F_B}{\frac{1}{2}\rho V^2 A_B}$$

In which V= characteristics mean reference velocity and A_B = characteristics area.

Basco and Adam summarize the results of the study for a nonsubmerged jump in a wide rectangular on a horizontal floor stated that;

- for free surface systems and a nonuniform flow field, the drag coefficient is dependent on the Reynolds number, Froude number, block geometry and also flow profile;
- the ratio of drag force to free jump, sequent depth, pressure force is the most practical force coefficient;
- the standard, Y-shaped and T-shaped blocks all produced similar forces under identical frontal projected areas.

Shterenlikht and Maslov (1984) studied on characteristics of the drag on baffle blocks by determine the relationship between the drag coefficient and, C_D (C_{xs} term is used in the paper) of baffle blocks and the kinematics characteristics of the flow and geometric parameters of the baffle platform. Three possible schemes of movement of the flow on the horizontal baffle platform were examined in the given investigations shown in figure 2.3 below.

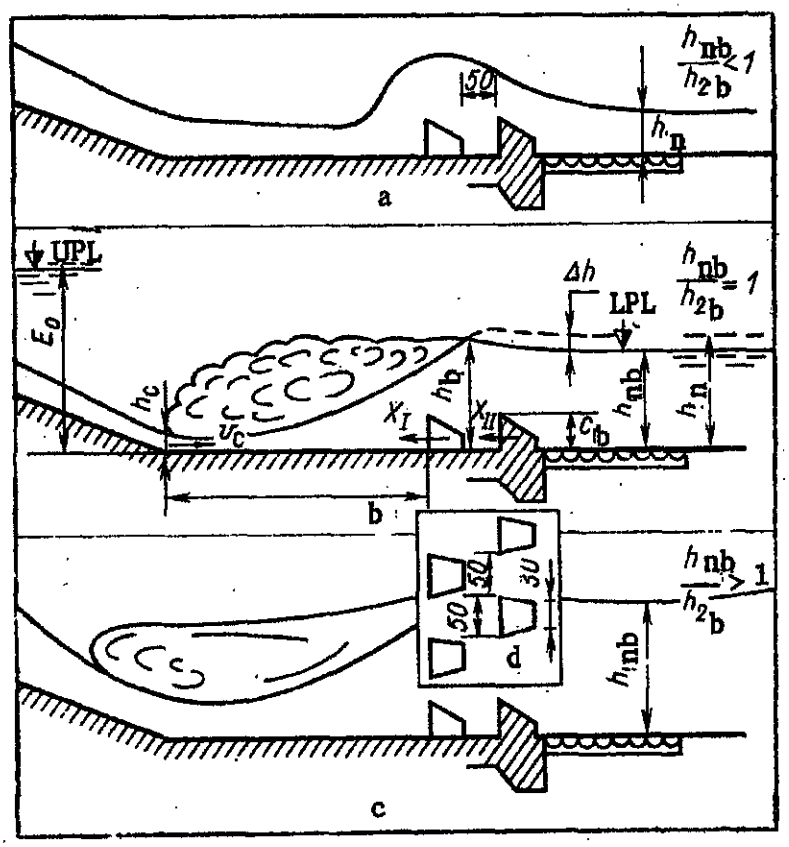

Figure 2.3: Schemes of flow on a horizontal platform with baffle blocks.

The scheme of the fluid flow regimes was realized during gradual submergence of the lower pool. A change in the regimes of the fluid on the platform leads to a change in the velocity characteristics of the flow, which ultimately affects the reaction of the baffle blocks. The results of direct measurements of the drag coefficients of the blocks C_{xs} as a function of submergence of the lower pool h_{nb}/h_{2b} on passing from the first flow scheme to the third are shown in figure 2.4 (h_{nb}/h_{2b} are the natural and second conjugate depths in the presence of baffle blocks on the platform).

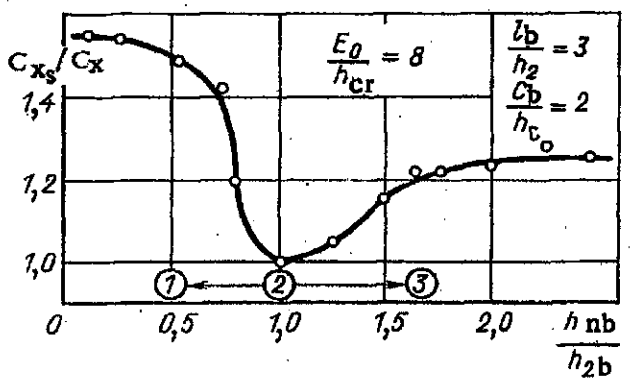

Figure 2.4: Graph of relative value of the drag coefficient C_{xs}/C_x as a function of a submergence of the lower pool h_{nb}/h_{2b} .

As could be expected, the maximum C_{xs} corresponds to flow past the blocks according to the scheme in Figure2.3 (a). As submergence h_{nb}/h_{2b} increases the drag coefficient of the block begins to decrease to a minimum value of C x. In this case the hydraulic Jump is in a limit state (Figure 2.3(b)). A decrease of C_{xs} from a certain peak value to a minimum corresponds to movement of the hydraulic jump toward the vena contracta. A further increase of the natural depth h_{nb} and transition to a submerged hydraulic jump is accompanied by an insignificant increase of the value of the drag coefficient of the baffle blocks. The indicated increase of the values of C_{xs} is a consequence of a slow increase of the average velocity of running against the block v r as submergence increases. Of greatest practical interest is the second scheme of flow on the platform (Figure 2.3(b)) corresponding to the minimum value of the drag coefficient of the baffle blocks. In this case the criterion of calculation of baffle blocks is the minimum value of their reaction corresponding to a jump in the limit state. Further result analyzed from the paper by Shterenlikht and Maslov is explained detailed in chapter 4.

CHAPTER 3

METHODOLOGY AND PROJECT WORK

3.1. Procedure

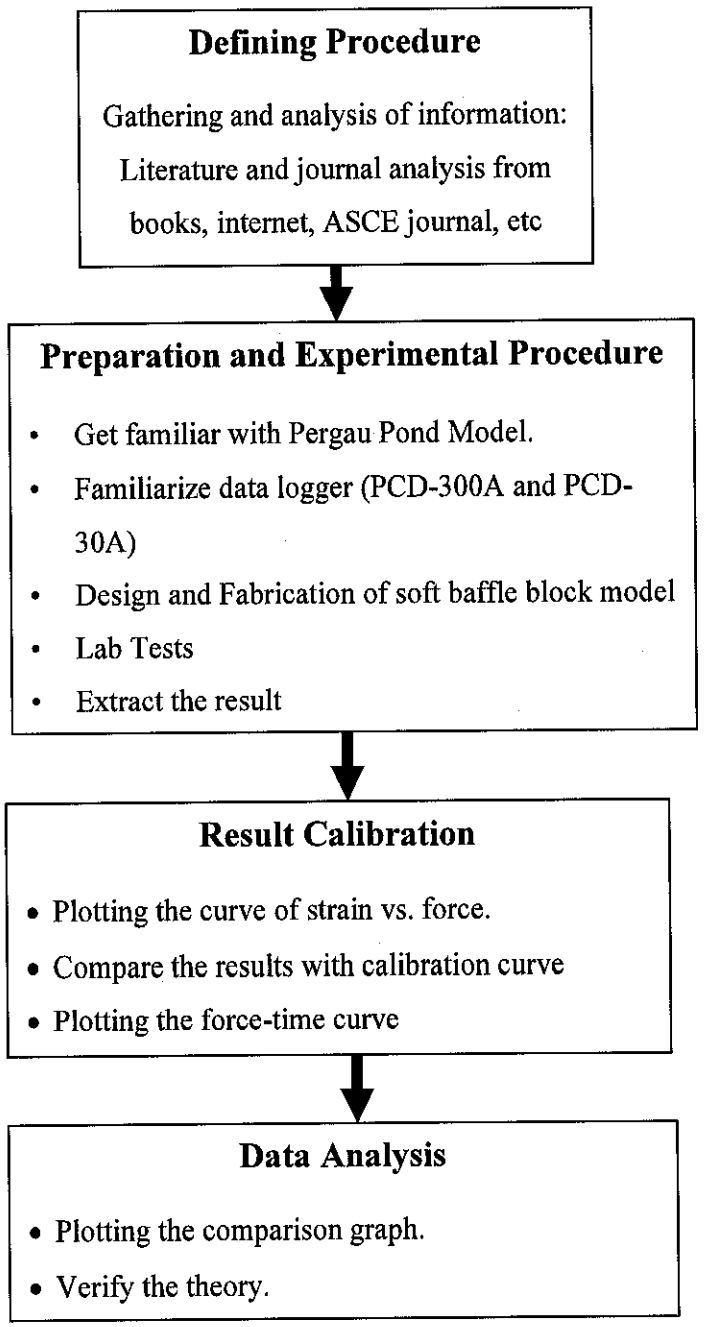

Figure 3.1: Project Flow Diagram

Figure 3.1 shows the project flow diagram which represents the complete process flow of the project.

3.1.1. Defining Procedure

Conduct a literature review and gathering the information of drag force on structures. Find out more information on the internet, books and journals available. The basic principles of flow condition in an open channel need to be understood by reading the book and review the existing research that conducted by other researcher example from ASCE transaction. All the information obtained are gathered and utilized for the purpose of this work.

3.1.2. Preparation and Experimental Procedure

Familiarize Data Logger (PCD -300A and PCD 30A)

Strain gages are designed to electrically detect the "strain", minute mechanical change occurring in response to applied force. They enable detection of imperceptible elongation or shrinkage occurring in structures. Measurement of such elongation or shrinkage reveals the stress applied to structures. KFW waterproof strain gage, which is manufactured in Japan, was selected for the measurement of dynamic strain mainly because they can be conveniently be applied to structures of varied materials and shapes. The strain sensor is 10 mm in diameter and approximately 0.2 mm in thickness. This foil strain sensor is protected with special plastic coatings on the surfaces to ensure outstanding water proof ness. It is usable for 100 hours or more under 10 MPa in water. Some other specifications of the gage are stated in table 3.1.

Table 3.1: Specifications of KFW waterproof strain gage

Gage pattern	: triaxial
Applicable linear expansion coefficient	: 23 x 10^{-6} /°C
Resistance	: 350 Ω
Operational temperature range	: -10 – 80 °C
Leadwire cable	: polyester-coated cooper wire

KFW gage is connected to KYOWA sensor interfaces PCD-300A series, which make the existing PC a versatile measuring instrument. The PCD-300A enables the PC to perform force measurement through the use of strain gages. Once sensors are connected, interactive operation on the PC enables measurement of strain data at a desired sampling rate. The control software PCD-30A enables the PC to control the sensor interfaces PCD-300A. Using the software, the PC sets measuring conditions and performs data acquisition, graph display and file conversion to CVS format on MS-Windows 98/2000/XP. If the direction of the principal stress is known in advance, a uniaxial gage aligning the sensitivity axis with the direction is needed. Then, the strain gage output expresses the principal strain. However, the direction of the principal stress is rarely known particularly in the present experimental study which involves turbulent flows. Thus, for stress analysis it is required to bond three strain sensors in three different directions as shown in figure 3.4. The 0^{o}/ 45^{o}/ 90^{o} triaxial gage produces strain readings in terms of ε_a, ε_b and ε_c, respectively.

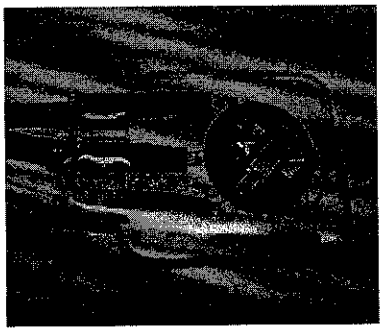

Figure 3.2: 3-axial strain gage

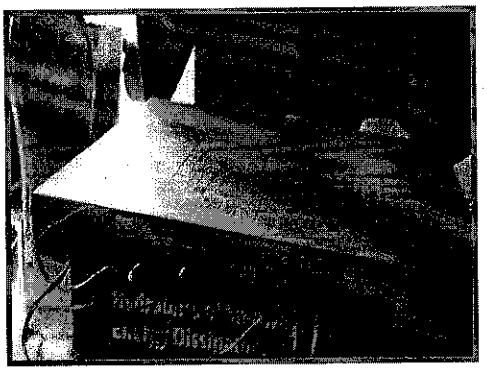

Figure 3.3: PCD-300A

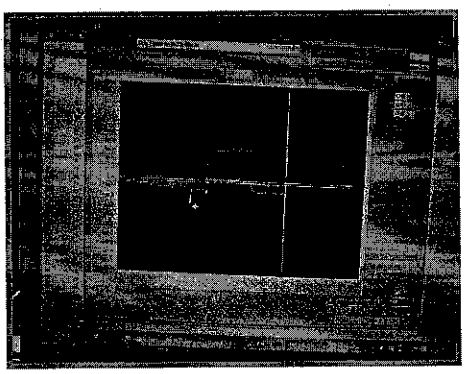

Figure 3.4: PCD-30A

Design and Fabrication of soft baffle block model

The two out of four soft baffle block model have been designed based on theories from [5, 12]. Followings are the list of block design involve in this studies;

1. Design 1: Standard USBR Trapezoidal Shape (3.7 x 5.5) cm.
2. Design 2: Standard USBR Trapezoidal Shape-actual structure (2.0 x 2.8) cm.
3. Design 3: Standard USBR Trapezoidal Shape (4.5 x 5.5) cm.
4. Design 4: Slope Trapezoidal Shape (5.0 x 5.5) cm.

Refer to Appendix A for overall dimension of each design.

Materials used to fabricate those soft baffle blocks model are sponge (cut into shape accordingly), covered by pieces of shaped transparency paper with help of strong glue and strong tapes. The reason of using a soft block model is because hard property materials belong to the wood is not allowed to detect the deformation of block surface due to load acting on it. Figure 3.7 below shows fabricated soft baffle blocks model which have been used in the lab tests.

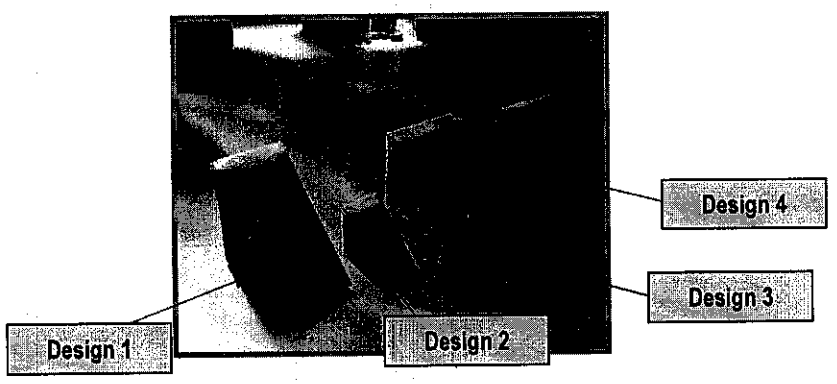

Figure 3.5: Soft baffle blocks model

Lab Tests

Total numbers of eight experiments have been run in Pergau Pond Model in UTP Laboratory. Two tests with different discharges (12 lit/s and 30 lit/s) for each design have been done. An experimental set up can be shown in figure 3.6 below. While recording the data, velocity and depth were also measured at every minute using a current meter. The lab tests have been conducted of average 30-40 minutes for each single test.

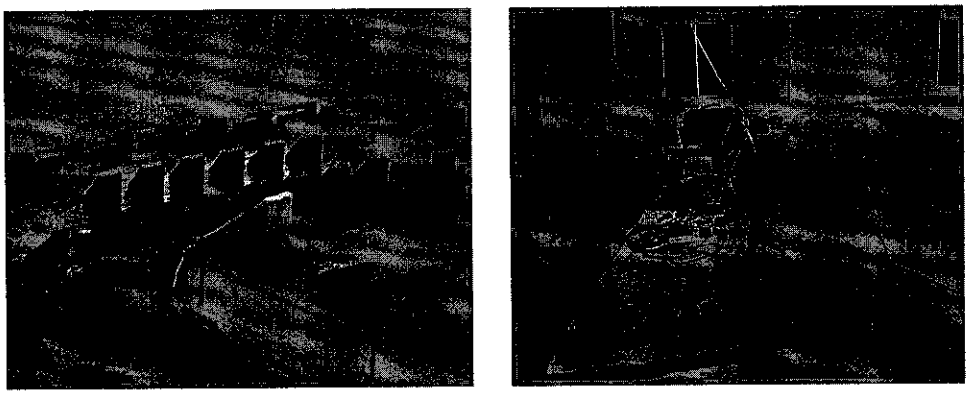

Figure 3.6: Experimental Setup

Figure 3.7: Velocity and Depth Measurement using current meter equipment.

3.1.2. Result Calibration

Results obtained are saved and graph of strain versus time is plotted. In order to obtain the value of forces exerted on the block, the data is calibrated using a special method of doing force-strain calibration. This procedure is done by putting a weight onto the soft baffle block model attached with the strain gauge, and its material deformation is recorded which is shown in figure 3.8 below.

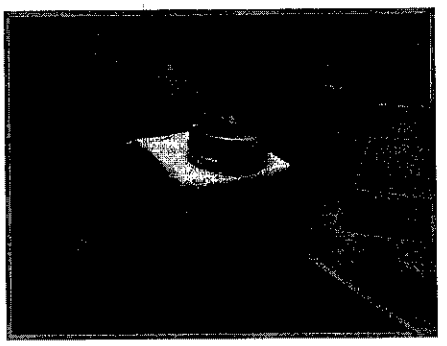

Figure 3.8: Strain-force Calibration work

The calibration graphs of strain- force of all block design can be shown in Appendix D. However, a few factors are considered to ensure the calibration procedure is close to accuracy and relevant value obtained. Those factors are:

1. **Location** – a weight is putted centrally onto the strain gauge assuming normal force acting on block at a maximum velocity value.
2. **Material Property** – the soft block model is soaked before the calibration, assuming the condition of material is the same as in a lab test.

From the calibration graph obtained, graphs of force- time are plotted according to the values shown thru the curves. Overall graphs of force-time can be referred to Appendix E.

3.1.3. Data Analysis

From the curves of force- time obtained, the comparison graphs based on factors considered are plotted. By using literature review as a reference, the theories of the results obtained are identified. During the analysis, some of data found containing errors which contributed to difficulty of verifying the theory. However, the basic parameters influencing drag forces performance can be identified.

3.2. Tools Required

i. **Mobile PC (Laptop)**
ii. **KFW waterproof strain gage** – To measure the dynamic strain applied to varied materials and shapes.
iii. **KYOWA sensor interfaces PCD-300A** – Makes PC a versatile measuring instrument.
iv. **Control Software PCD-30A** – Enables the PC to control the sensor interfaces PCD-300A.

CHAPTER 4

RESULT AND DISCUSSION

This chapter provides the result and discussion on the basic parameters affecting the drag force on baffle blocks performance. The basic parameters such as shape, dimension, discharge and velocity factors are compared. Plotted graphs have been done to show clearly the result obtained and comparison made.

4.1. Drag Force Analysis

4.1.1. Effect of Height and Dimension of baffle block

Dimension effect

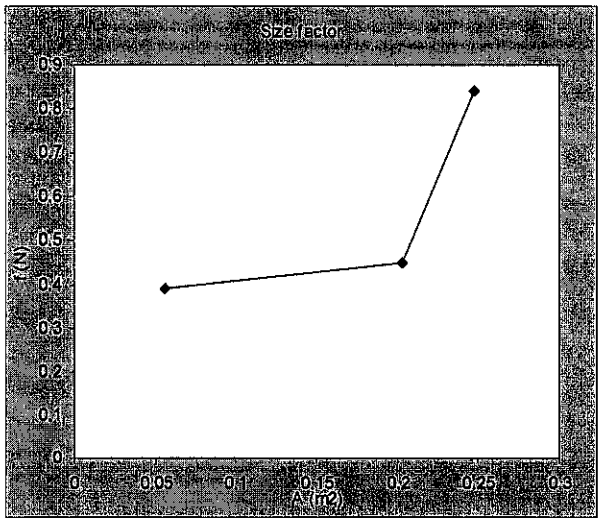

Figure 4.1: Force comparison graph of various dimension of standard USBR baffle block.

Refer to figure 4.1, graph of force vs. time is plotted based on result obtained from experiments and calibration graphs of each baffle block type. The specifications of the test are shown in table 4.1;

Table 4.1: Specifications of experiment results

Block Type	Trapezoidal		
Figure	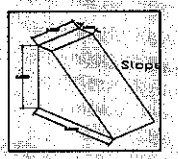		
Flow rate (lit/s)	12		
Initial depth (cm)	4.7		
Froude No. range	0.27 – 0.32		
Dimension and Area	**Design**	**Dimension (cm)**	**Frontal Area(cm^2)**
	Design 1	3.7 x 5.5	20.35
	Design 2	2.0 x 2.8	5.6
	Design 3	4.5 x 5.5	24.75

A figure 4.1 shows a curve of effect of a frontal area to the total drag force. In stable condition of flow, the higher the frontal areas, resulting in higher value of drag forces. The drag forces also increasing with increment of Froude number, Fr_1. For the size and dimension comparison, only a standard USBR block shape is considered to avoid influences of the shape factor. Graph of experimental result comparing the forces varies with time between the various dimensions of blocks can be shown in Appendix E. From the graph, a resultant rapid behavior of forces is due to fluctuating of turbulent flow.

Baffle Block height effect

For this study, height of block is fix makes limited parameter are analyzed due to time constraint. However, based on studies by Basco (1971) he measured the horizontal force component F_B on the blocks and expressed it in terms of a force

coefficient, Φ. Figure 4.2 below shows that, force coefficient is increase with increasing of height of block, h.

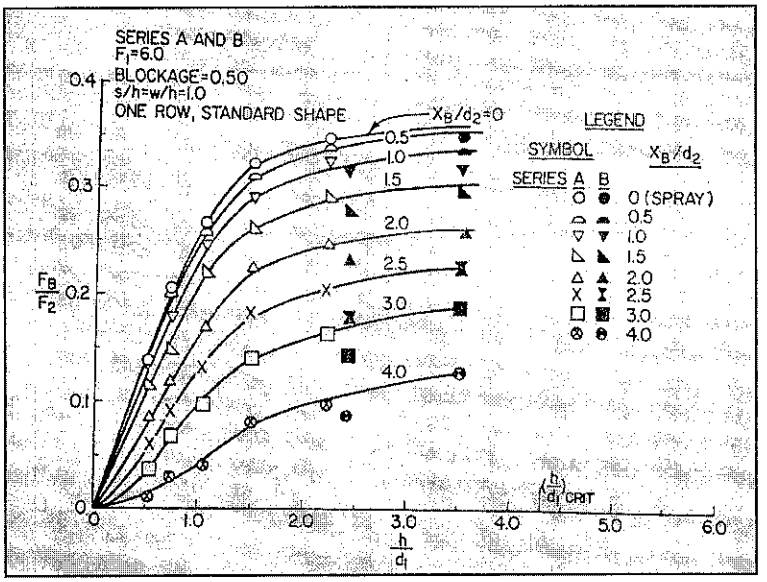

Figure 4.2: Force ratio versus height ratio at $Fr_1 = 6$

4.1.2. Effect of Velocity and Discharge

Discharge effect

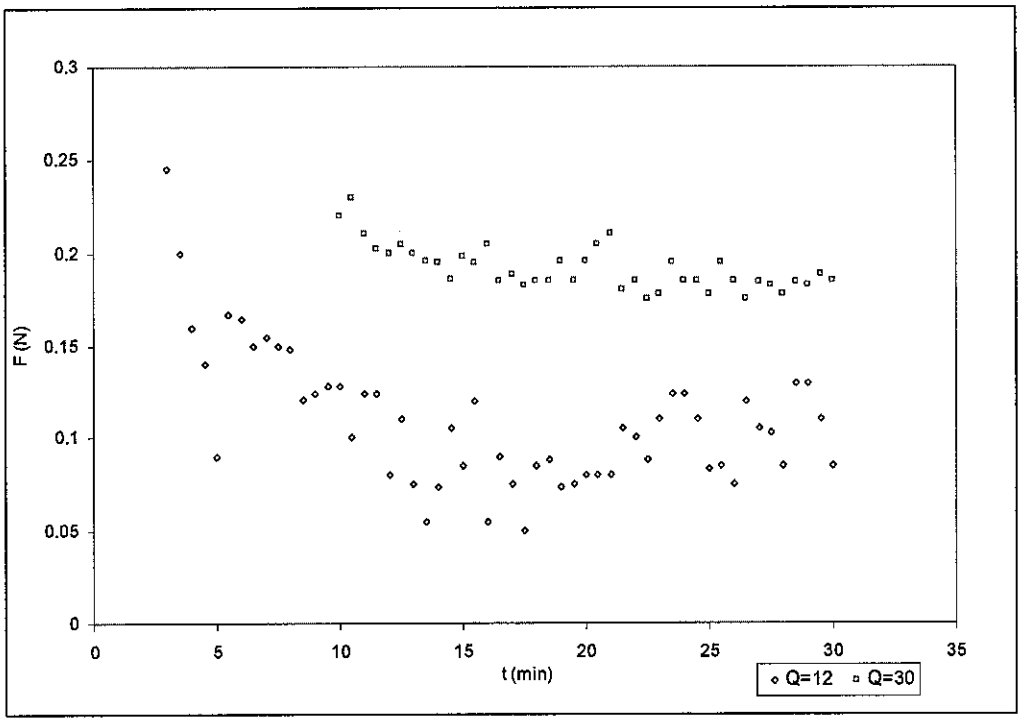

Figure 4.3: Force comparison of different discharge of Design 1

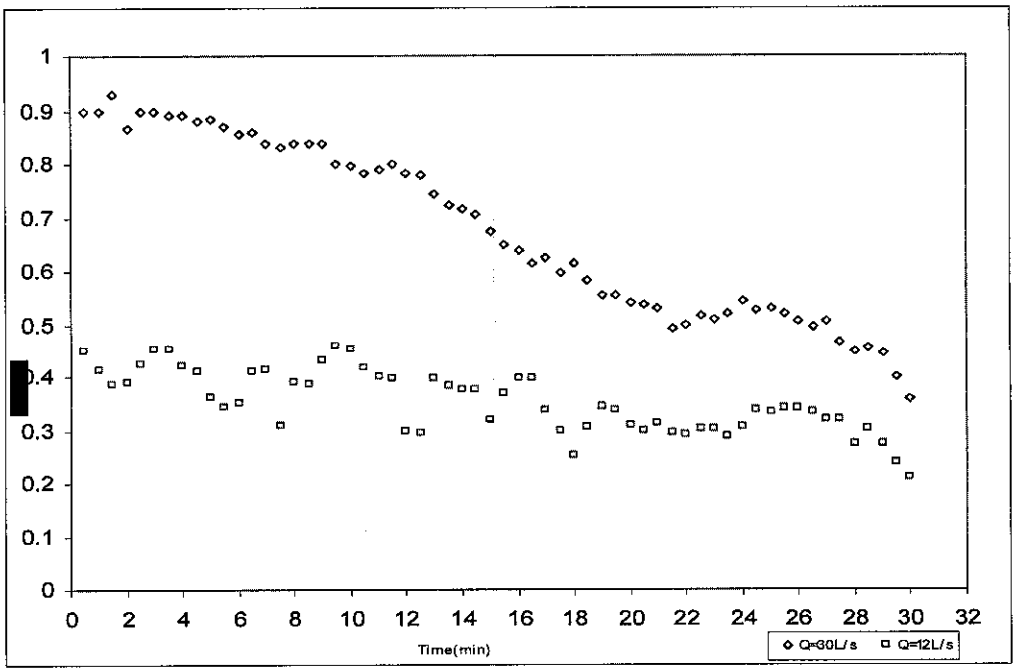

Figure 4.4: Force comparison of different discharge of Design 2

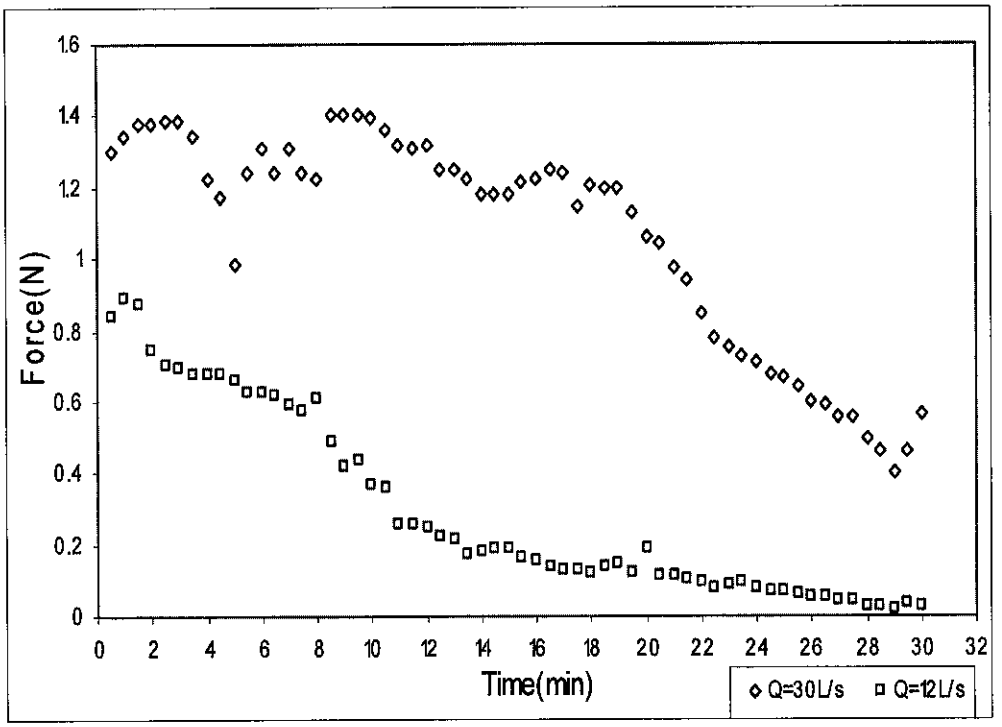

Figure 4.5: Force comparison of different discharge of Design 3

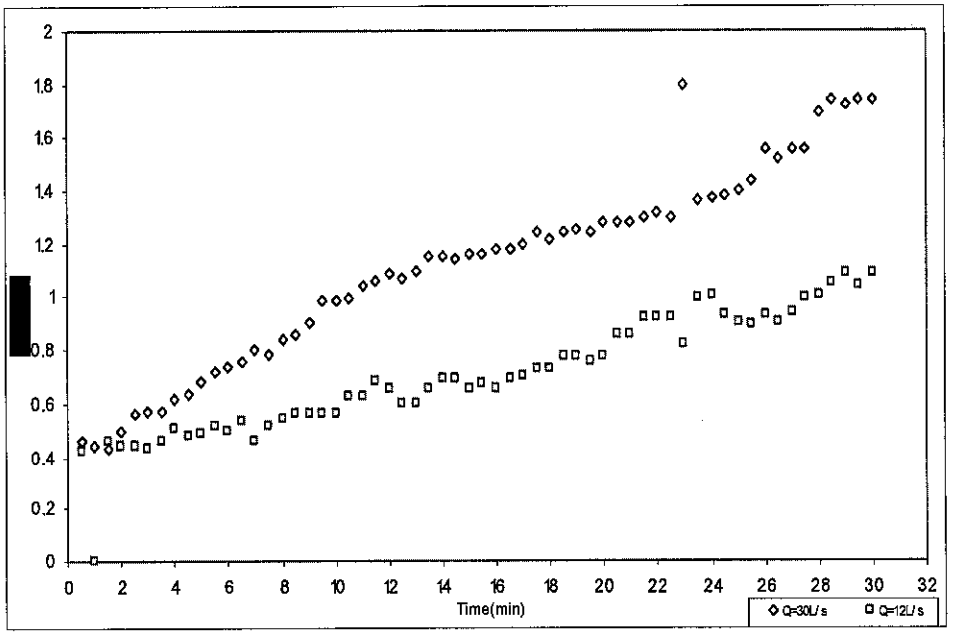

Figure 4.6: Force comparison of different discharge of Design 4

Referring to figure 4.3 to 4.6, the graphs of force vs. time obtained from experiments and calibration graphs for two different discharges of each design. Generally, flow

rate of 30 lit/s gives higher value of forces compared to 12 lit/s. An increment of drag forces is linear with discharges of flow [17].

Generally, all the graphs line seemed to give an increment and decrement of total force varies with time which is an error of the experiments (refer to **part 4.5** for detail error justification). However, a resultant rapid behavior of forces is due to fluctuating of turbulent flow (*refer to figure 4.7*).

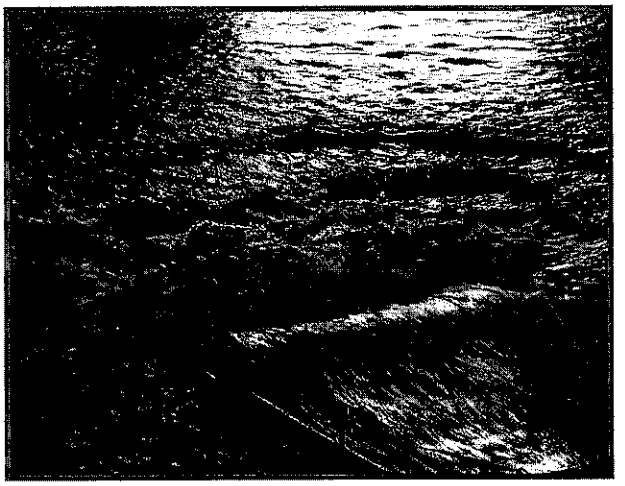

Figure 4.7: Fluctuating of flow

Velocity Effect

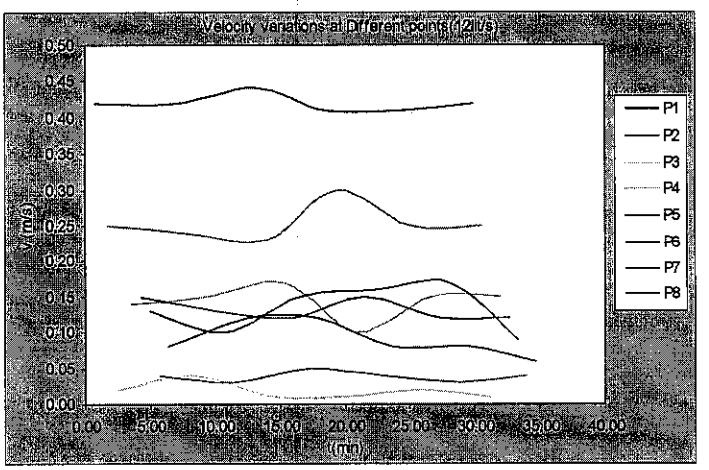

Figure 4.8: Velocity variations of Design 3 blocks (12lit/s)

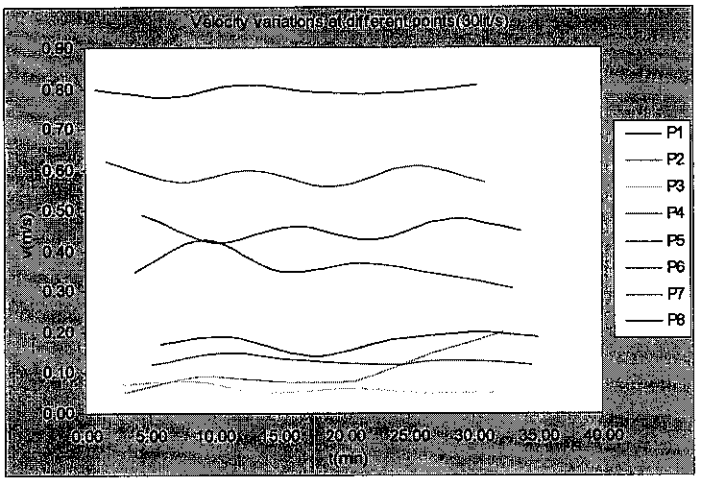

Figure 4.9: Velocity variations of Design 3 blocks (30lit/s)

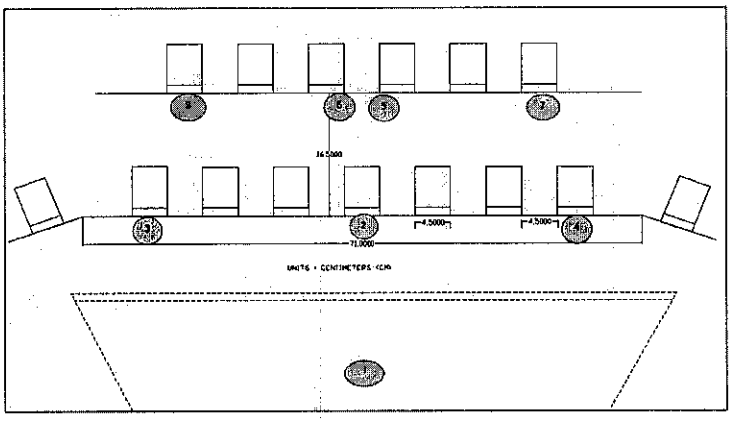

Figure 4.10: Locations in stilling basin of velocity measurement

Figure 4.8 and 4.9 above show the velocity variation at different points in Pergau pond model stilling basin. Both curves (Discharge of 12 lit/s and 30 lit/s) present that the velocity at the centre line give higher value compared to other points. Point 1 gives exact highest value since the flow is directly flow from a tunnel (jet flow). Point 2 gives lower velocity value after flow is crossed a weir structure located along the stilling basin (*refer to figure 4.10*). Referring to the graphs, velocity at point 3, 4, 7 and 8 give a lower velocity value compared to the points at a centre line. This is because, at point 3 and 4, the flow experienced more diverging while point 7 and 8 have less diverged but more energy is dissipated resulting in low velocity values. In drag force analysis, point 2 which has a great velocity value is analyzed. Curve which shows a velocity factor effecting total of drag forces is illustrated in figure 4.11 below;

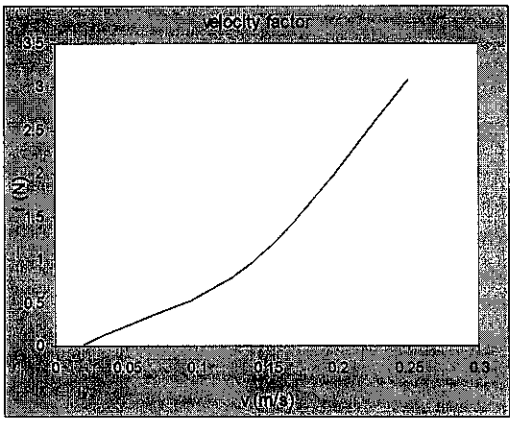

Figure 4.11: Velocity factor effecting total drag force.

Based on figure 4.11 above, it is proved that an increment of velocity value increased total drag forces. The graph is plotted by considering the velocity measured in the first row of baffle blocks at point 2, 3 and 4 and theoretically drag forced is calculated. Shterenlikht and Maslov (1984) has investigated the effect of water depth with respect to velocity and force. He found that velocity and drag force are decreased with increment of water depth. In this study, the depth of the water is insignificant makes the data cannot be extracted for comparison purposes. In addition, the Pergau pond model having the inlet and outlet structure which the experiment has began at the equilibrium state (equilibrium is a condition where $water_{in} = water_{out}$). Overall result of velocity and depth measurement linear with time can be shown in Appendix G.

4.1.3. Relative Position of Baffle Block

In this study, baffle block location of whole experiments is set by making use of existing fix location. This parameter is not modified and investigated due to limited equipment and time constraint. However, Basco (1971) studied the effect of varies location of block in a stilling basin. He found that for any given block height, the force is large if the block is close to the toe location and decrease as the distance between the toe and the block increases. He also found that the force is increase with increment of blockage and moving the second row closer to the first row. His findings are illustrated in figure 12 and 13 below.

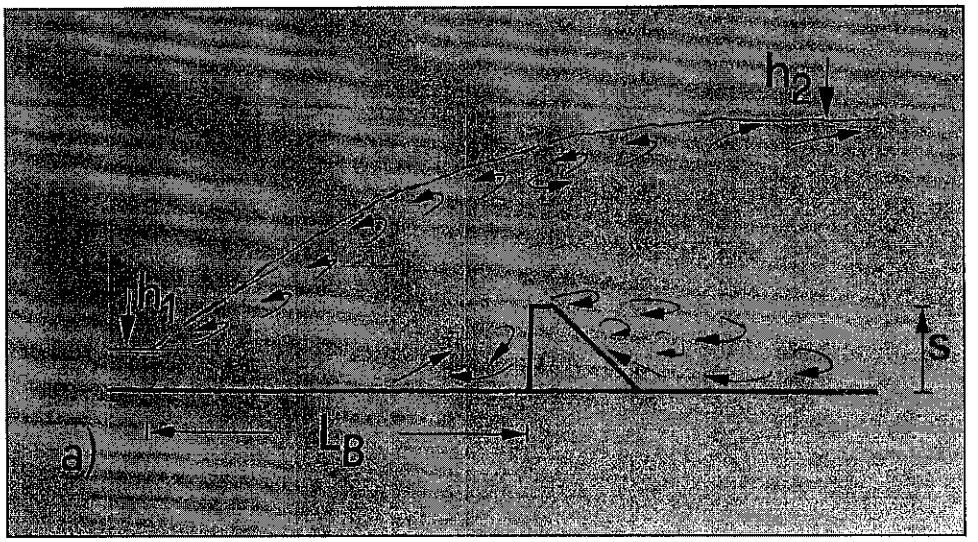

Figure 4.12: Side view of baffle block basin

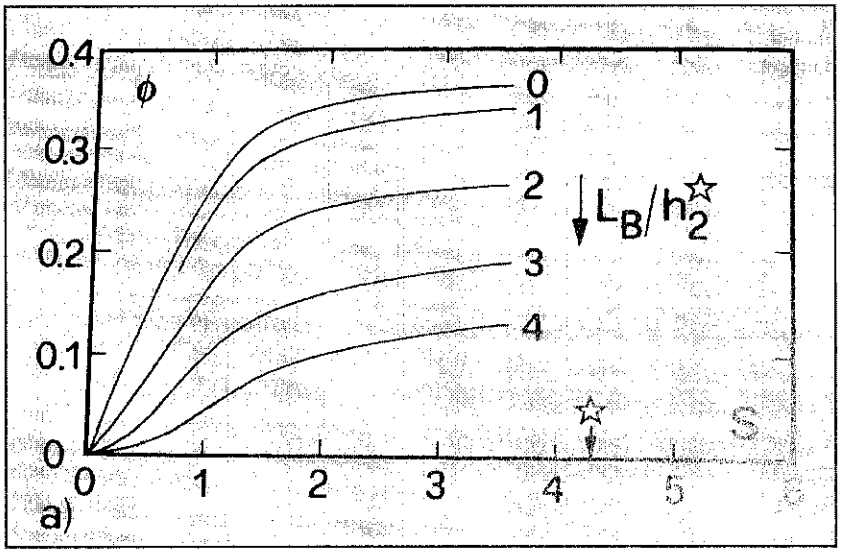

Figure 4.13: Drag force (Φ) with various toe position

From his investigation, he has generated the equations of optimum block height and optimum block position as illustrated below;

$$S_{opt} = 1 + \frac{1}{40}(F_1 - 2)^2$$

$$\left(\frac{L_B}{h_2^{\,2}}\right)_{opt} = 1.6 + 7.5\,F_1^{-2}$$

As a result, the optimum block height S_{opt} increases and optimum block position relative to the block front decreases with increasing approach Froude number. Therefore, the force coefficient increases with F_1 as

$$\Phi = \frac{1}{7} + \frac{1}{100} F_1$$

4.1.4. Effective shape of baffle block.

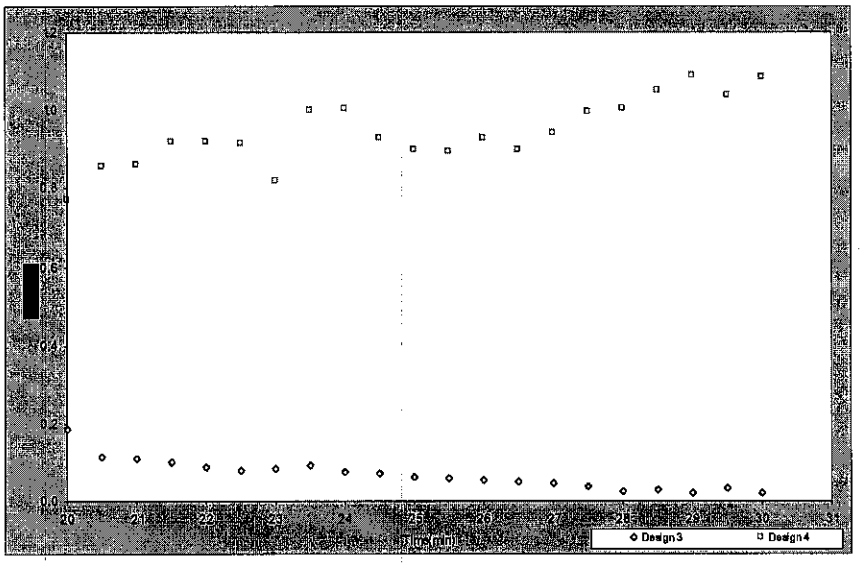

Figure 4.14: Force comparison graph of design 3 and 4 of 12 lit/s

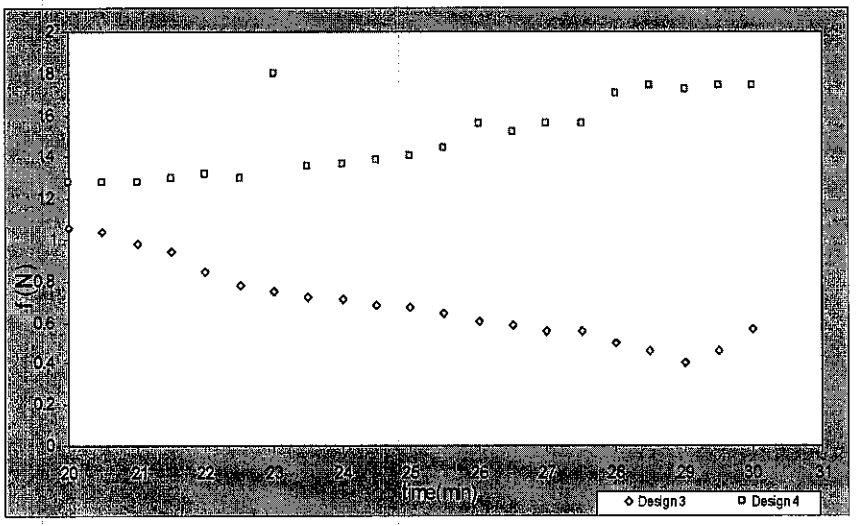

Figure 4.15: Force comparison graph of design 3 and 4 of 30 lit/s

According to the figure 4.14 and 4.15, the pattern of comparison is slightly the same which both curves of each flow are increasing for design 4 but decreasing for design 3. Design 3 and 4 are compared because the total frontal areas between the blocks are not much different. From the graph presented, it shows that baffle block of design 3 gives lower force compared to design 4, but there are possible causes due to decrement and increment of the values respectively. Rather than equipment error, it is thought to be the shape of sloped trapezoidal (design 4) itself contributed to the resulting changes. Figure 4.9 shows clearly the differences between the shapes in 3-dimension view.

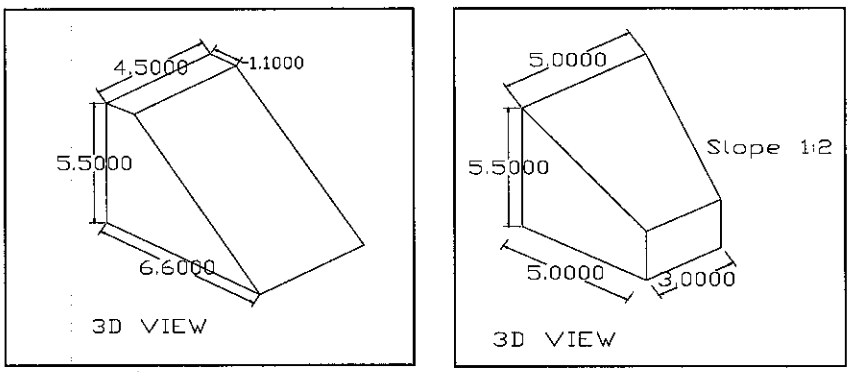

Figure 4.16: 3-dimensional view of design 3 and design 4

When flow exerted forces onto the blocks, a block of design 3 still can attain the loads due to the longitudinal width of 1.1 cm owned, while a block of design 4, the force is keep increasing because the tip of the block has experienced continuous deformation without any back- up of longitudinal width which resulting in deflection of the object.

This experiment result can be supported by previous studies regarding the baffle block optimum shape. Following are the general findings on blocks by previous researcher;

1. The optimum block front face is vertical and perpendicular to the approach flow, the block corner is sharp.
2. Baffle blocks are prone to cavitations damage and should not be used for approach velocities above 20m/s.
3. Standard baffle block like the trapezoidal USBR block should be used.

4.2. Drag Force Coefficient

Drag force coefficient is an important parameter in drag force analysis on block where it is convenient dimensionless parameter considering factor of upstream velocity and the size, shape and orientation of the body. In this study, the coefficient of drag forces is not investigated due to unavailability of equipment. However, previous investigation are analyzed and studied. Shterenlikht and Maslov (1984) studied the characteristics of the drag on baffle blocks. His findings supported an equation of drag coefficient as below;

$$C_D = \frac{F_D}{\frac{1}{2}\rho V^2 A}$$

From the investigation, he found that a value of C_D increase as the baffle blocks approach vena contracta after they found that kinetic energy losses is increase in through- flowing jet of the jump with distance to the vena contracta. He also found that a decreasing of relative height of the baffle block C_b /h_c leads to an increase of C_D as shown in figure 4.17 (a) and 4.17(b) below;

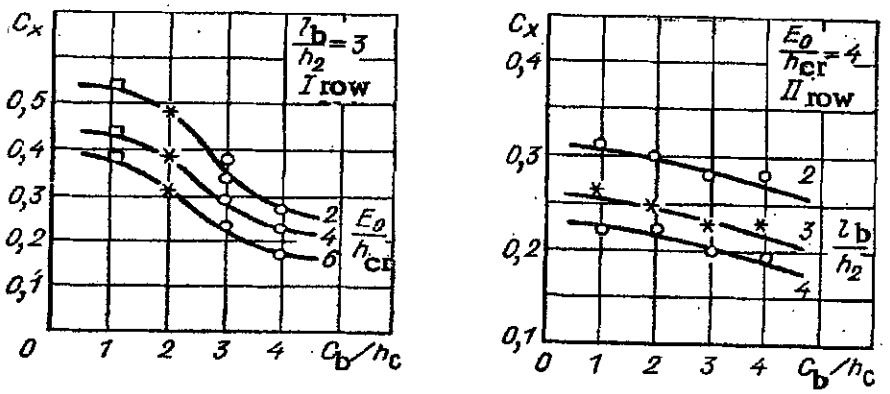

a) b)

Figure 4.17: Effect of block height on drag coefficient; a) First row, b) Second row

From the figure 4.17, the range of drag force coefficient for row 1 and row 2 is approximately 0.15 to 0.55 in various height of block. This result has proved the hydraulic guideline *on Hydraulic Theory*, (1991) which has recommended that drag coefficient of 0.6 for row 2 and 0.4 of row 1 is used. Besides, he also found that an increment of depth and Fr_1 result in increment of C_D.

4.3. Error Justification

There are many factors contributed to the errors identified in the results above. Obvious error encounters are listed as below;

- Increment and decrement of forces varies with time.
- Inaccuracy value of resultant forces.
- Measured velocity value.
- Unidentified data.

There are several factors that believe causing errors in the experiment results. Followings are the major causes of errors and its justifications;

(1). Equipment Error

a. Strain Gauge

- **Consistency:** a strain gauge has experienced an electronic drift phenomenon where the equipment having a thermal loss (heat) and it has increased with time changes. The device is become hotter resulting in lower efficiency of the equipment. Thus, it gives inconsistent data due to unstable system of the device.
- **Function and Arrangement:** The ideal strain gage would change resistance only due to the deformations of the surface to which the sensor is attached. However, in real applications, temperature, material properties, the adhesive that bonds the gage to the surface, and the stability of the metal all affect the detected resistance. Because most materials do not have the same properties in all directions, knowledge of the axial strain alone is insufficient for a complete analysis. Poisson, bending,

and torsional strains also need to be measured. Each requires a different strain gage arrangement [18].

b. Current Meter

- **Size:** the size of current meter available in the lab is oversize and not really suitable with water depth analyzed in the study. Bigger the current meter, higher the distraction of the flow resulting in inaccuracy of velocity reading. Thus, it affects the final result of analysis.
- **Handling equipment:** during measurement, there was no other equipment support the current meter standing. Thus, resulting in inaccuracy of depth measurement.

(2). Material Error

a. Soft Block Model

- **Calibration activity:** the soft block is soaked before the weights putted. However, actual water content seep thru the model is unpredictable. Inequality of water content in a model between calibration and experiment result in lower accuracy.

CHAPTER 5

CONCLUSION AND RECOMMENDATIONS

5.1. Conclusion

The factors affecting the drag forces on a baffle block were analyzed. Higher frontal area, A, and block height will provide higher drag forces, F_D. Higher flow rate of water, Q, results in higher drag forces, F_D. Also, higher velocity, V, will provide higher drag force, F_D. Standard USBR shape baffle block gives optimum value of drag forces, F_D, compared to sloped Trapezoidal shape block. From previous studies, drag coefficient, C_D is increase if the height of block decreases depth of water increase, distance of block to vena contracta increase, and Fr_1 decrease. Optimum size and type of shape of baffle block are required to improve the drag forces on baffle blocks exerted by the flow as well as effectively dissipate the energy. The factors affecting total drag forces on baffle blocks in a stilling basin were studied and understood. However, limited equipments and methods available and error occurred prevent the study accomplished as expected.

5.2. Recommendations

Through this project, the basic factors such as shape, dimension, discharge and velocity effects on drag force on baffle blocks were studied using a unique calibration method. Instead of using a strain gauge equipment to get a force value, it is strongly recommended that the force transducer is implemented to get more accurate value. Effect of arrangement and variable geometry of baffle blocks need to be investigated to get better future design. This can be achieved by using appropriate equipment and proper methods. If more parameters affecting the drag force on block are studied, the magnitude and behavior of drag forces on baffle block in a Pergau Pond stilling basin can easily be identified.

REFERENCES

[1]. David R. Basco, John R. Adams, "Drag Forces on Baffle Blocks in Hydraulic Jumps" in *Journal of the Hydraulic Division : Proceedings of the American Society of Civil Engineers*, pp.2023-2035, December 1971.

[2]. D.V Shterenlikht.; A.B. Maslov.; "Characteristics of the Drag on Baffle Blocks," in *UDC 627.838,* No. 6, pp.24 - 26 , June 1984.

[3]. Eduard Naudascher; "Chapt 2:Fluctuating and Mean Hydrodynamic Forces," in *Hydrodynamic Forces, Hydraulic Design Manual, A.A Balkema, USA* Vol 3, pp.1 – 125, 1991.

[4]. Daniel L.Vischer; Wili H.Hager; "Chapt 5: Stilling Basin," in *Energy Dissipators, Hydraulic Design Manual, A.A Balkema, USA* Vol 9, pp.61 – 78, 1995.

[5]. EM 1110-2-1603; "Hydraulic Theory," Chapt 2, pp. 1-16, Jan. 1990.

[6]. J. Pablo Porras VelÃ¡zquez ; " Physical Model Study of Hydrodynamic Forces Acting on Baffle Blocks ," of *IHE Delft Articles, Costa Rica*, May 2002.

[7]. Dan Naout, Iehisa Nezu, Hiroji Nakagawa,; " Hydrodynamic Behavior of Partly Vegetated Open Channels," *Journal of Hydraulic Engineering* ,pp. 625-633, 1996.

[8]. R.M Khatsuria, Micheal D. Meyer.; " Chapt 20 : Hydraulic Jump Stilling Basin," in *Hydraulic of Spillway and Energy Dissipators,* Marcel Decker. New York, pp. 388-434, 2005

[9]. R.M Khatsuria, Micheal D. Meyer.; " chapt 17 : Design of Spillway and Energy Dissipation for Flood Control Storage and Conveyance System," in *Hydraulic of Spillway and Energy Dissipators,* Marcel Decker. New York, pp. 672-736, 2005.

[10]. Saiedi S.; Kalaikumar V.; "Lessons from Design and Construction of a Hydraulic Model for Energy Dissipation and Erosion Studies," of *University Technology of PETRONAS*, May 2006.

[11]. Henk van Beijeren 1 and J. R. Dorfman2; "Kinetic Theory of Hydrodynamic Flows," in *Journal of Statistical Physics, Vol. 23, No. 4, 1980*

[12]. D. V. S. Verma1; Arun Goel2; "Development of Efficient Stilling Basin s for Pipe Outlets," *in Journal of Irrigation and Drainage Engineering*, May, June 2003.

[13]. DiMassamo, Robert A; "Hydrodynamic Forces on the Cavitation Free-Baffle Pier," thesis *presented at Boston, Mass..*in 1956.

[14]. Herleman, Donald R.F; "Effect of Baffle Piers on Stilling Basin Performance," *Journal, Boston Society of Civil Engineers*, Vol. 42, No. 2, April,1955,pp. 84-99.

[15]. Newman, James B., and LaBoon, Frank A., "Effects of Baffle Piers on the Hydraulic Jump," thesis *presented at Boston, Mass..* in 1953.

[16]. Anderson, Alvin G., and Dahlia, Warren Q., "Hydraulic Studies of the Spillway for the Mangla Dam," *Project Report No. 74, St. Anthony Falls Hydraulic Laboratory, University of Minneapolis, Minn..*Feb, 1968.

[17]. R. Narayanan and L. Schicas, "Force on Sill of forced jump," *Journal of Hydraulic Division, ASCE*, July, 1980.

[18]. <http:www-omega.com/literature/transactions/volume3/strain.html>

APPENDICES

APPENDIX A

BAFFLE BLOCKS DIMENSION

DESIGN 1

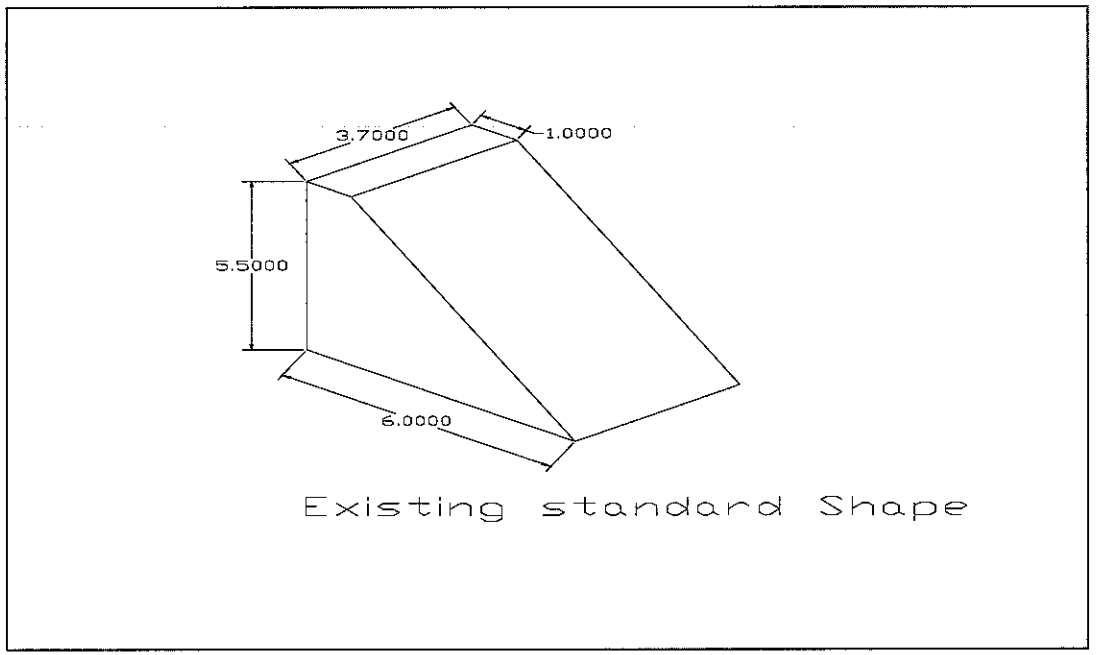

DESIGN 2

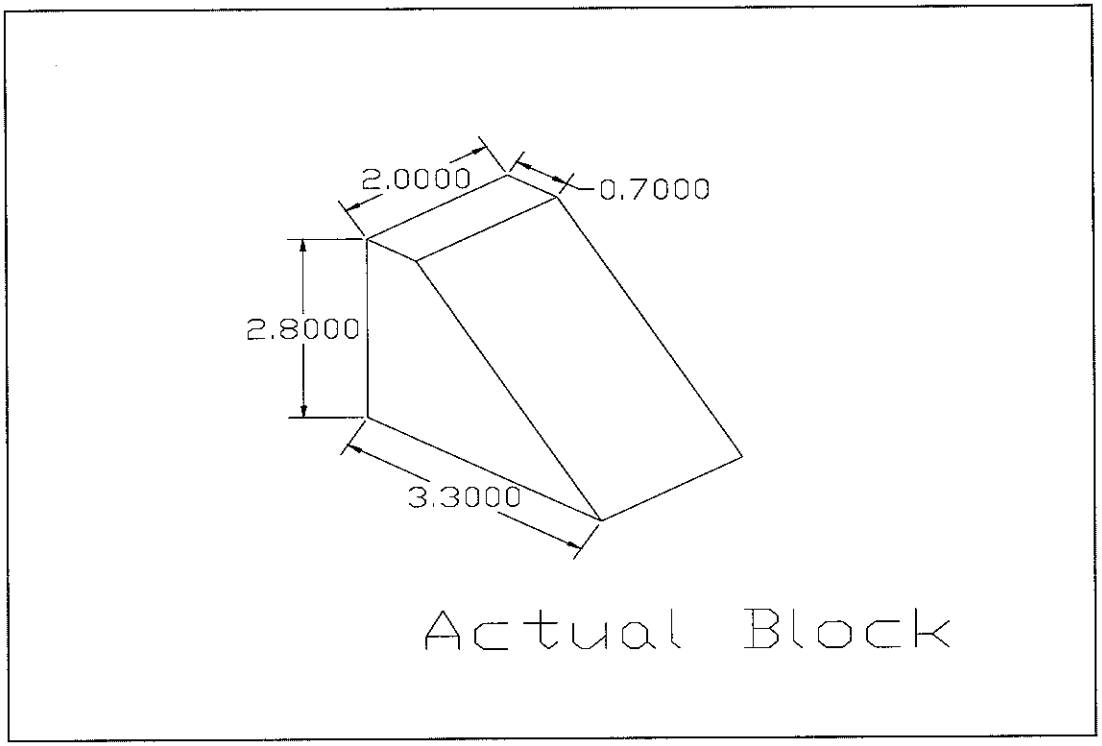

DESIGN 3

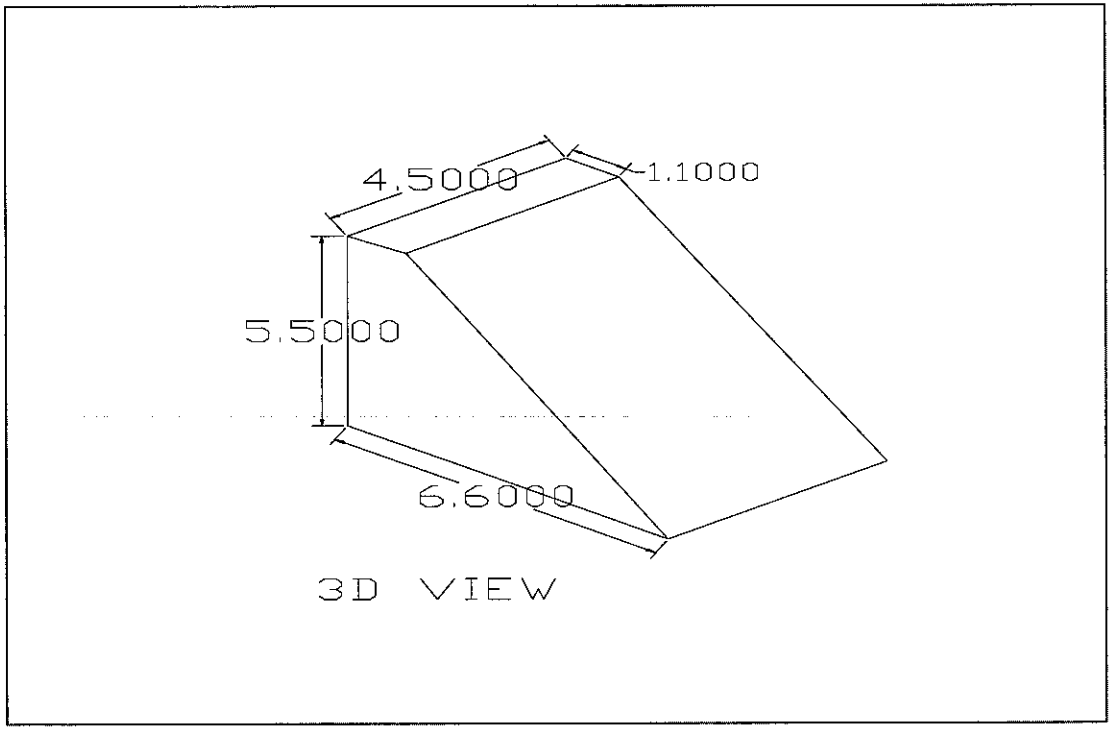

DESIGN 4

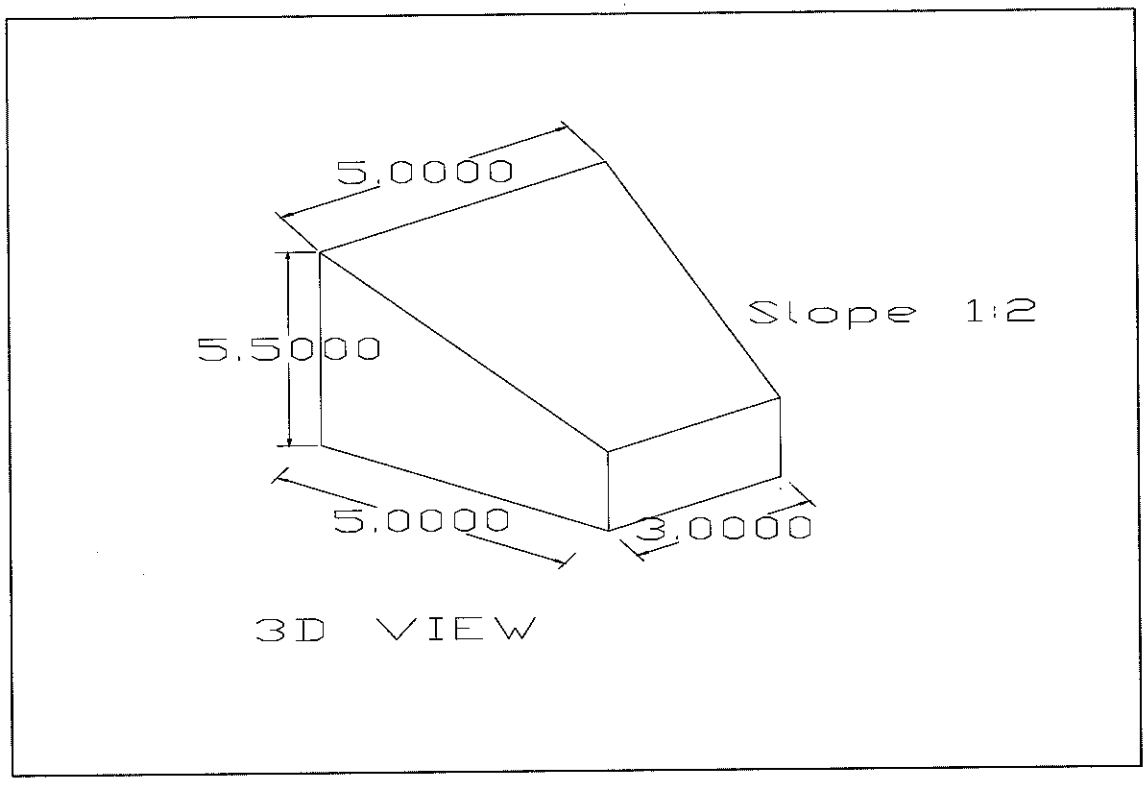

APPENDIX B

BAFFLE BLOCK ARRANGEMENT

DESIGN 1

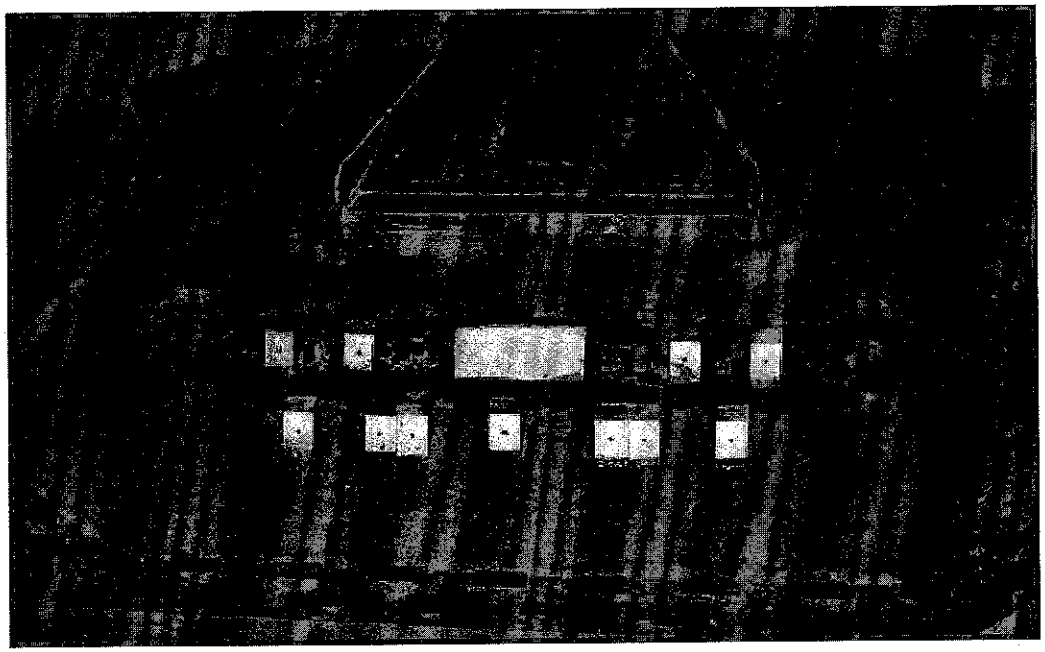

BAFFLE BLOCK ARRANGEMENT

DESIGN 2

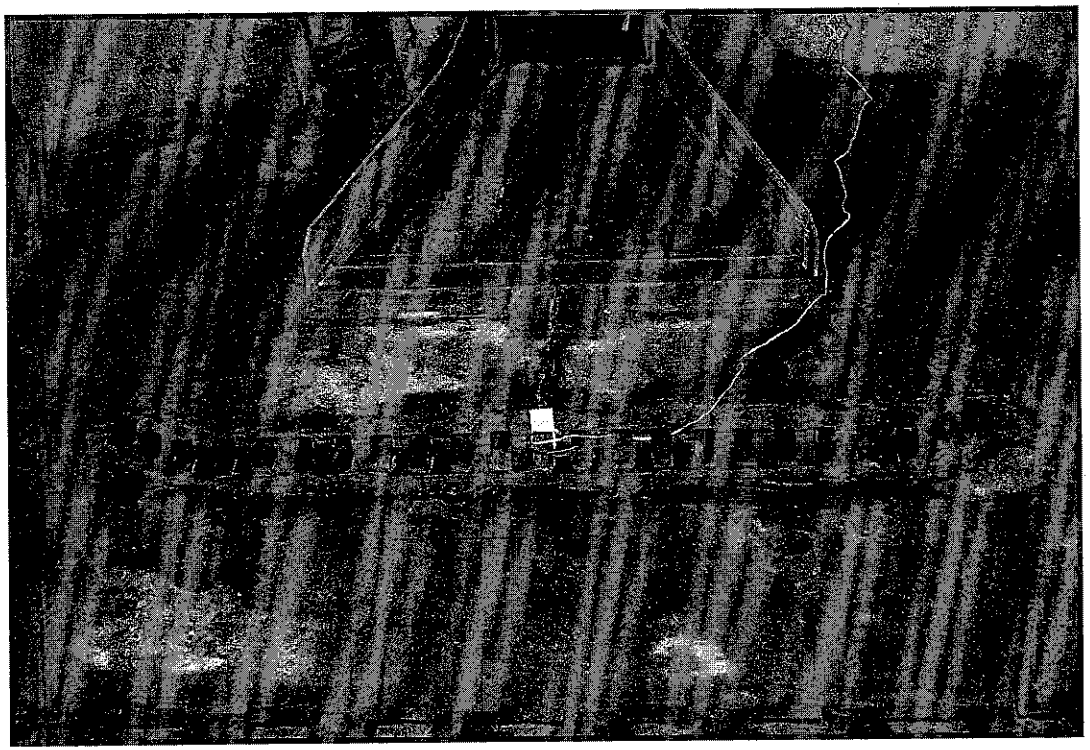

BAFFLE BLOCK ARRANGEMENT

DESIGN 3

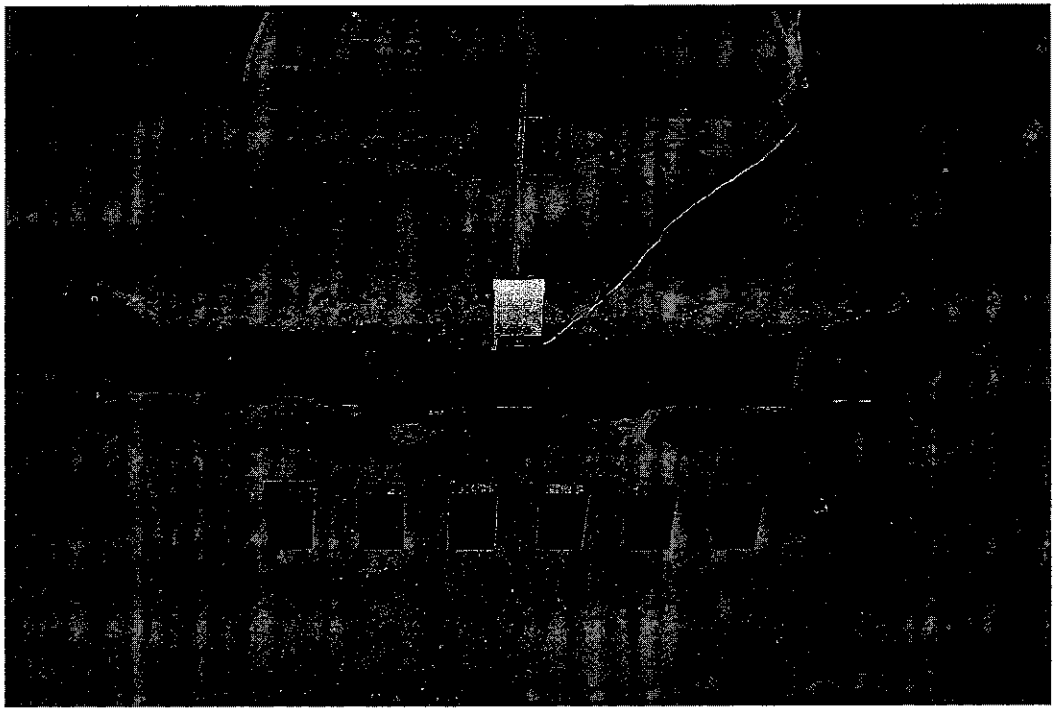

BAFFLE BLOCK ARRANGEMENT

DESIGN 4

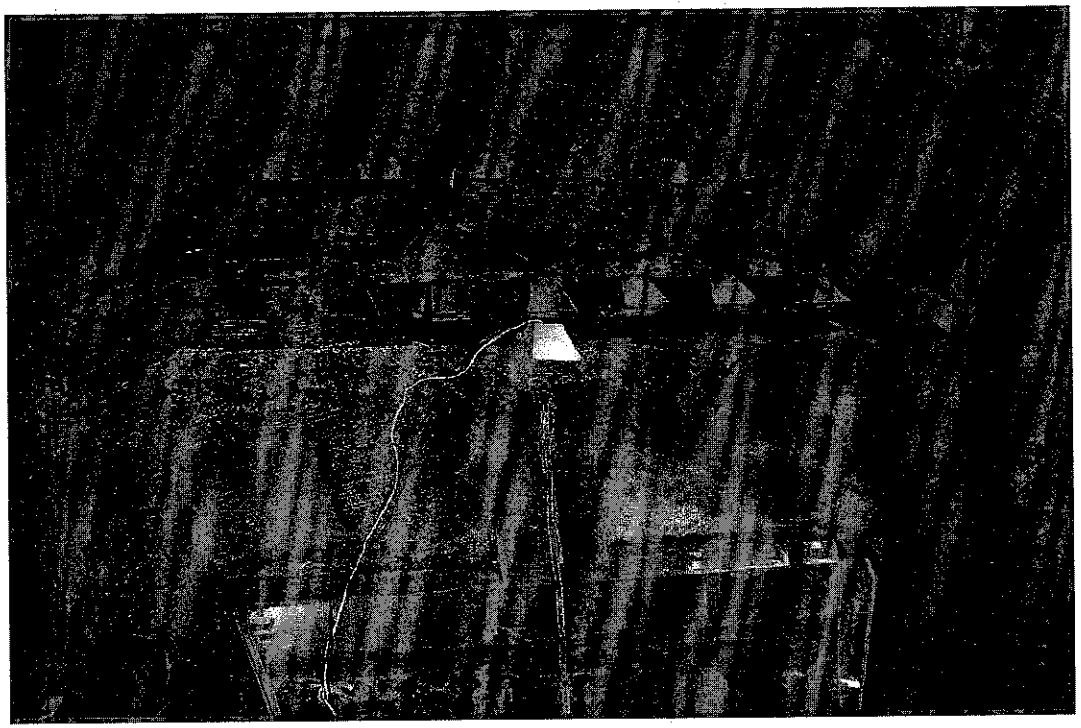

APPENDIX C

STRAIN- TIME GRAPH

DESIGN 1

A) Q= 12 L/S

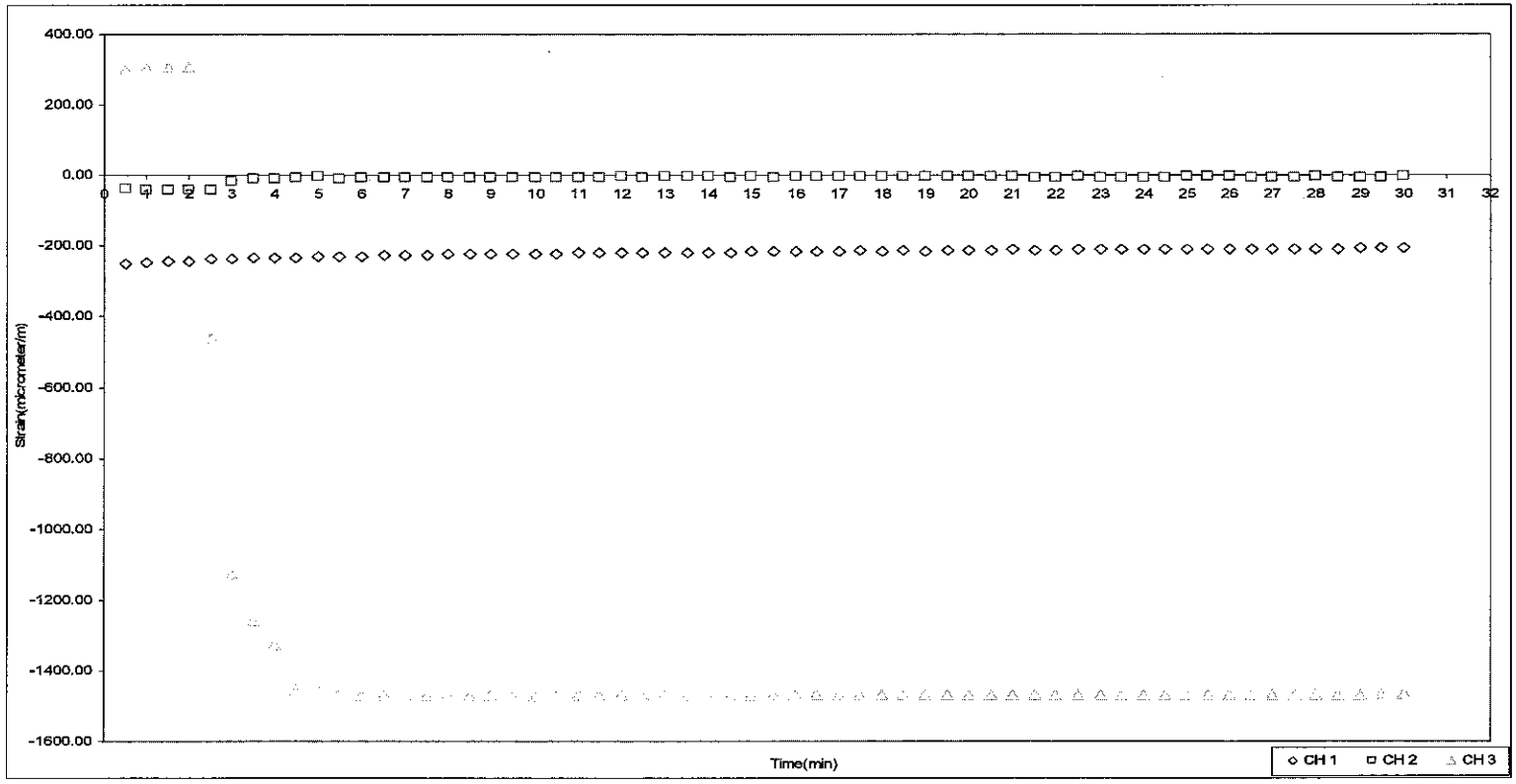

STRAIN- TIME GRAPH

DESIGN 1

B) Q= 30 L/S

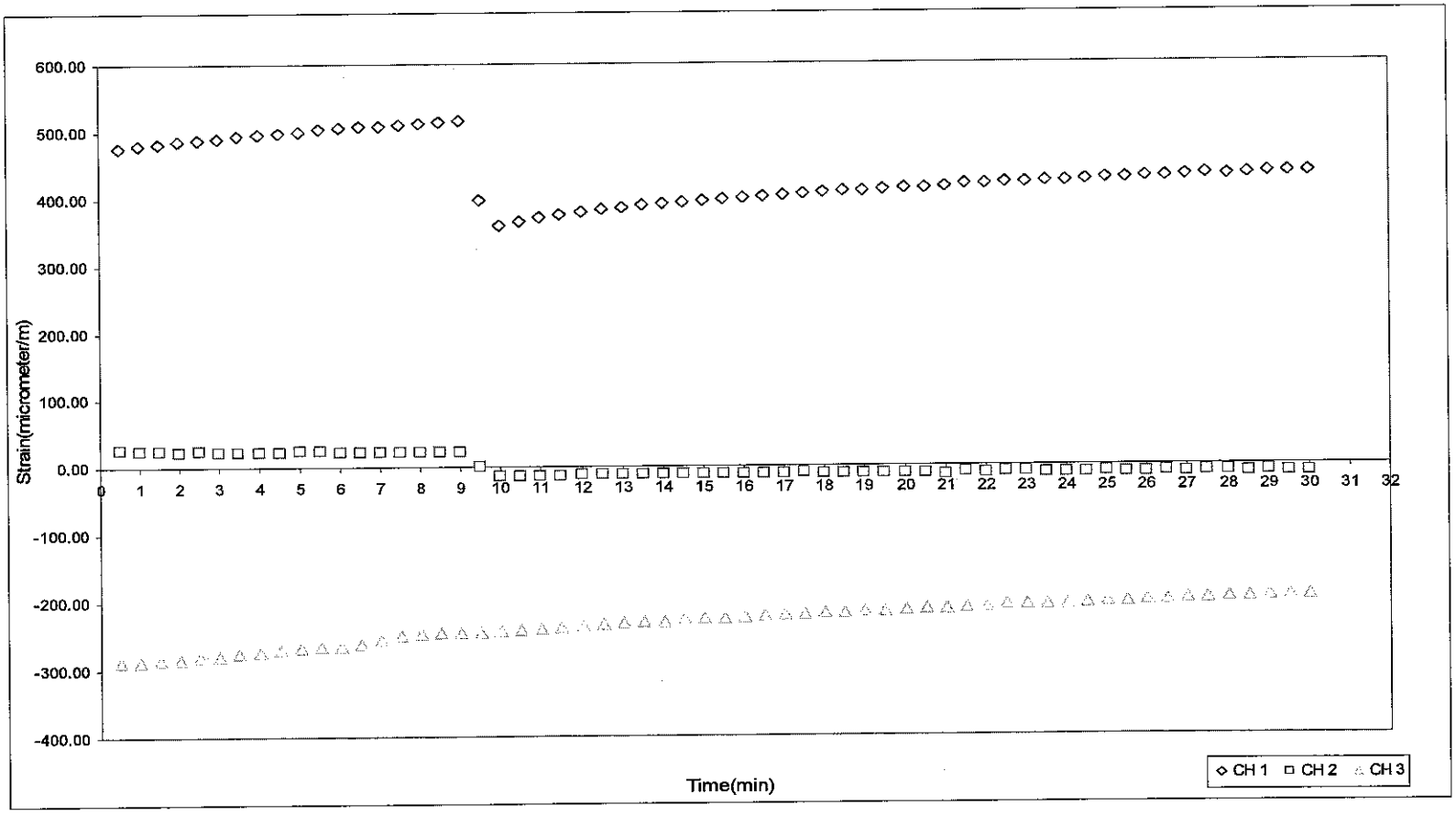

STRAIN- TIME GRAPH

DESIGN 2

A) Q= 12 L/S

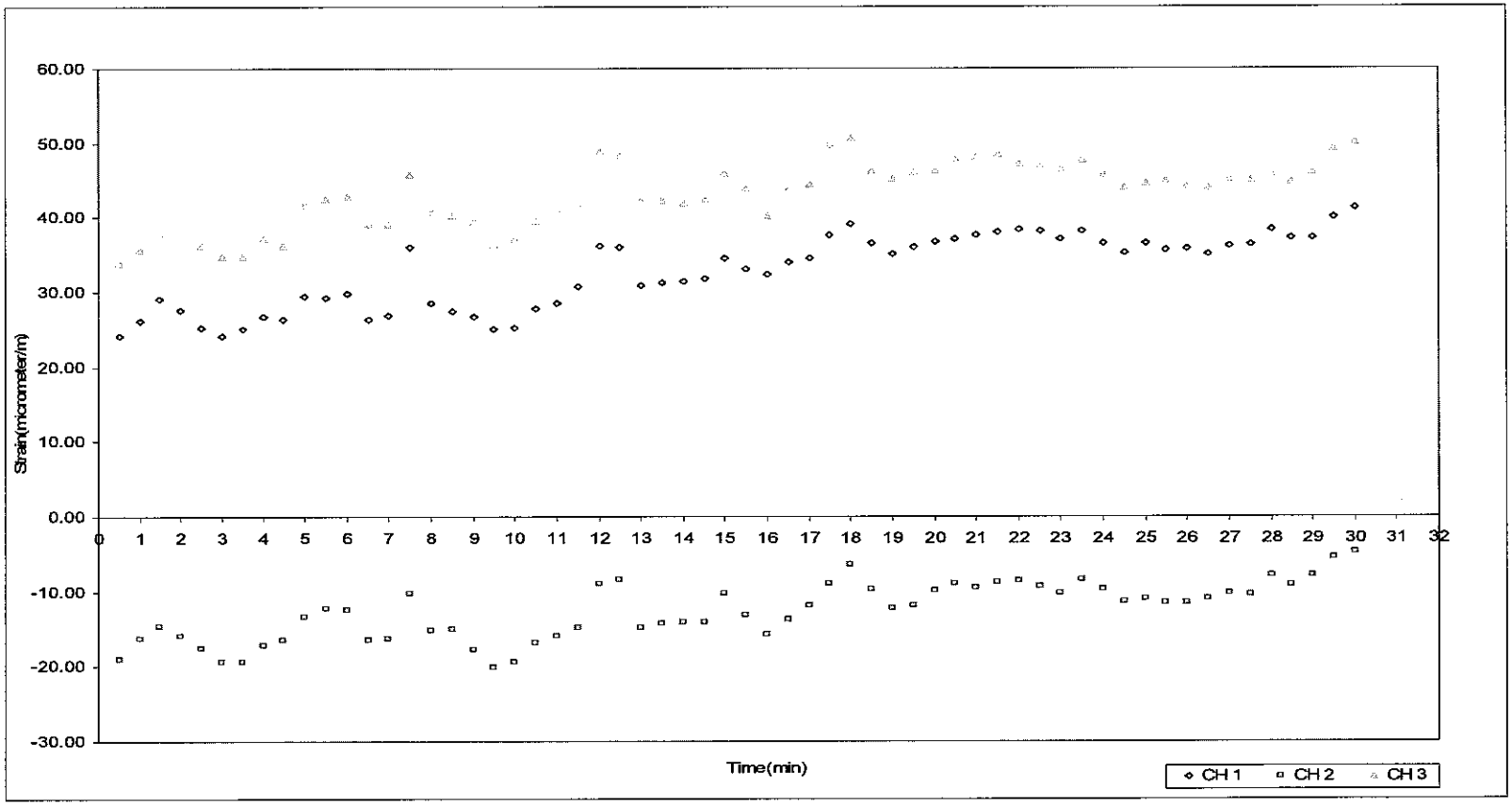

STRAIN- TIME GRAPH

DESIGN 2

B) Q= 30 L/S

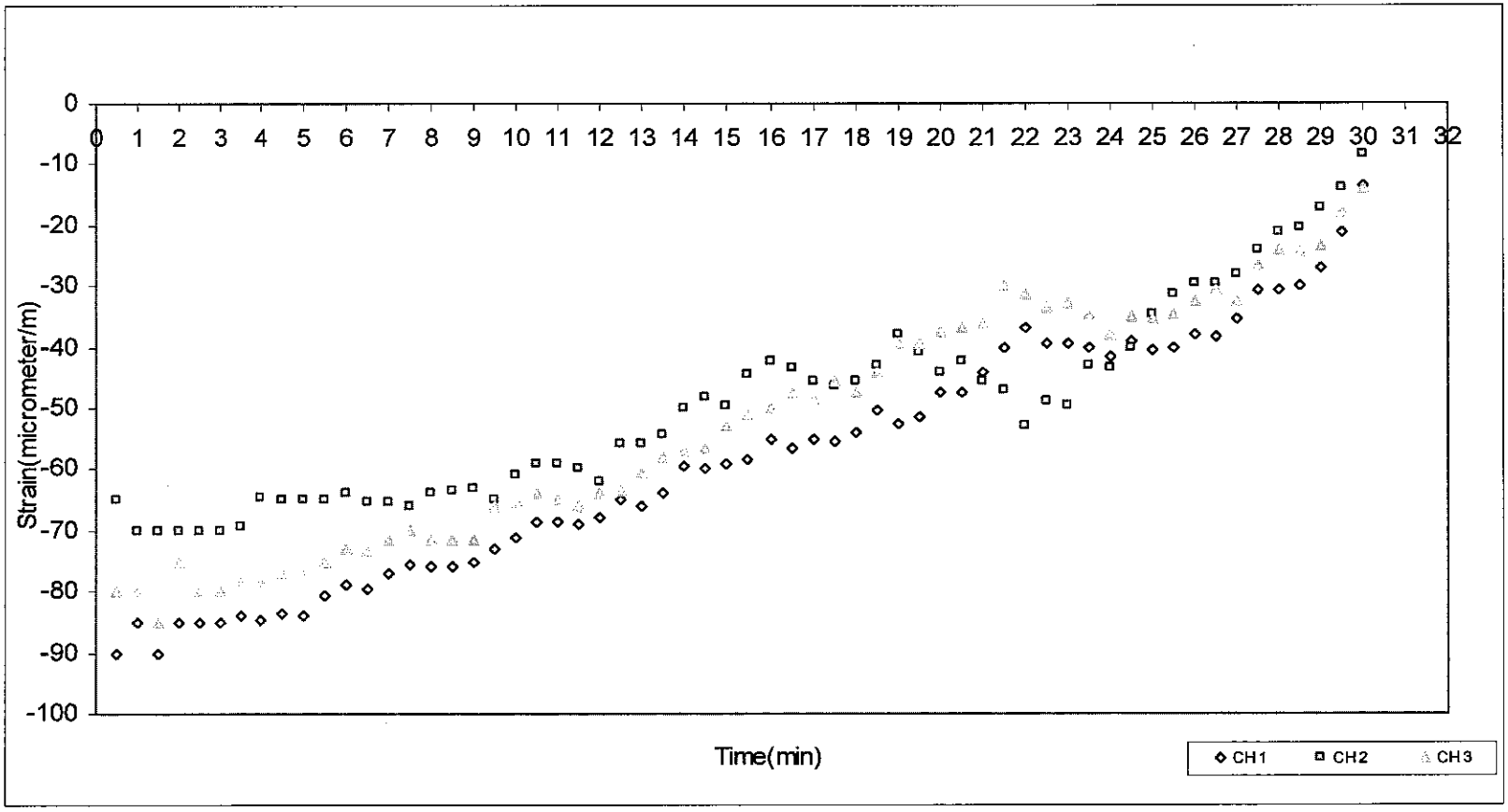

STRAIN- TIME GRAPH

DESIGN 3

A) Q= 12 L/S

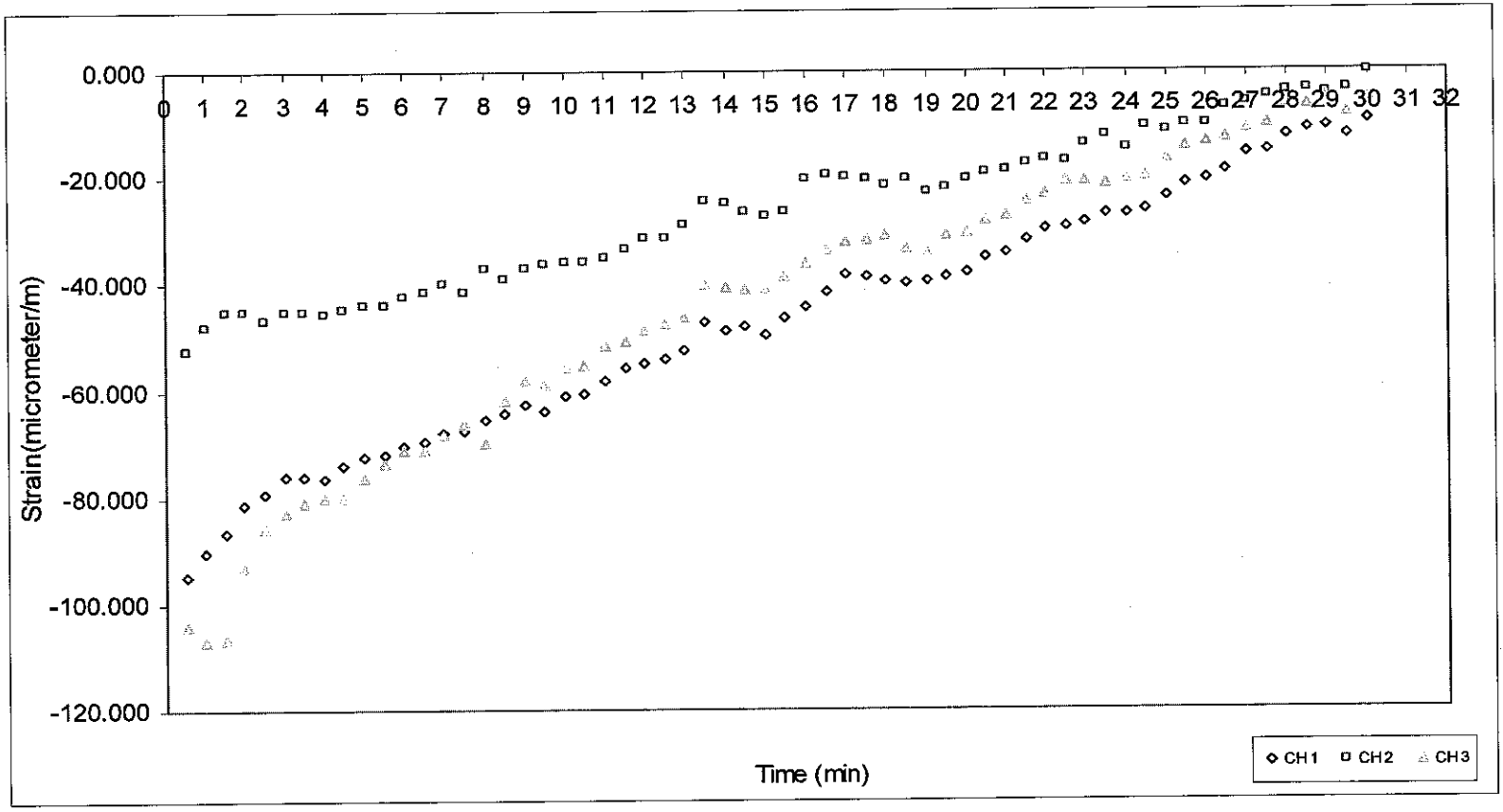

STRAIN- TIME GRAPH

DESIGN 3

B) Q= 30 L/S

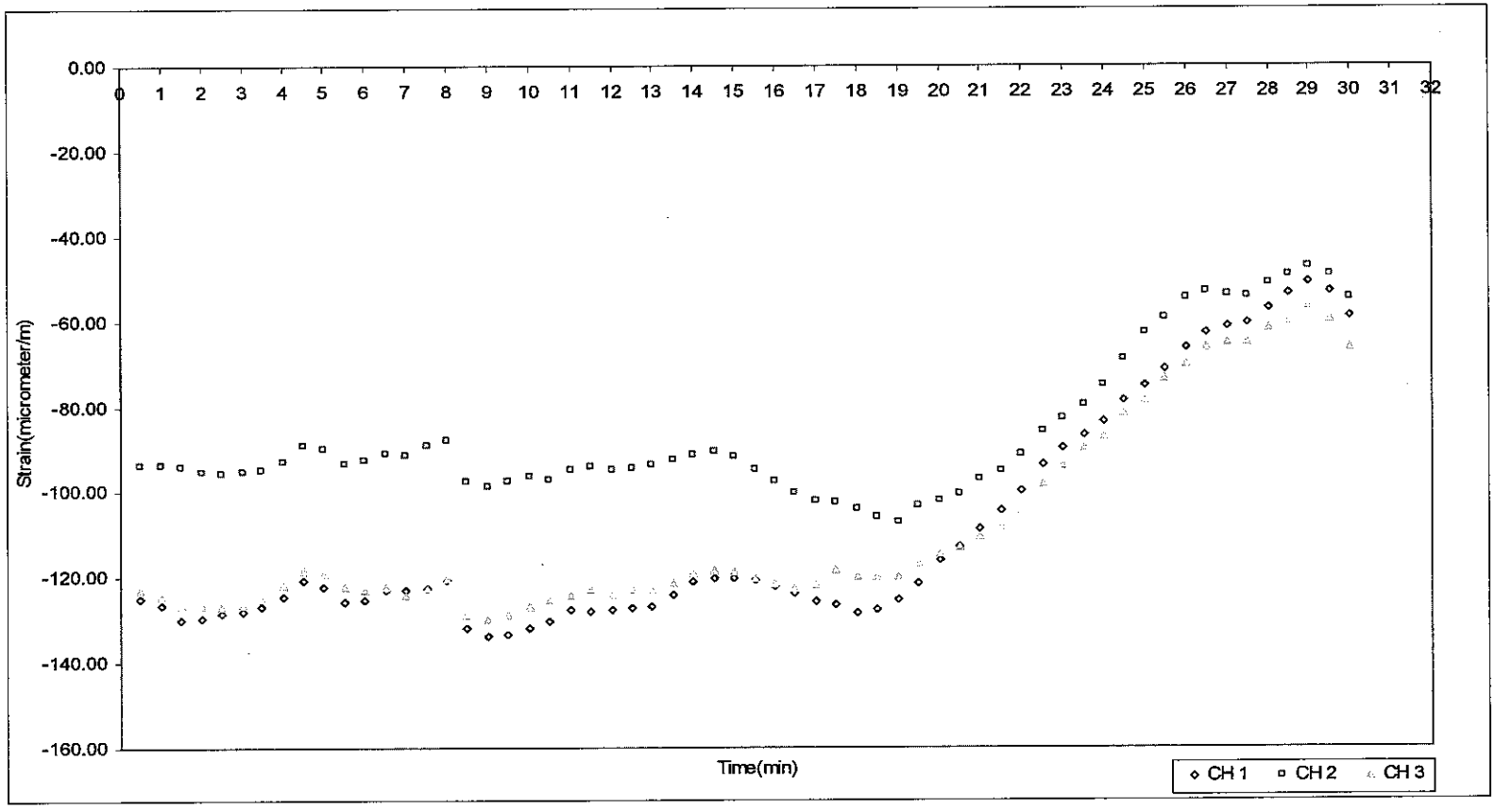

STRAIN- TIME GRAPH

DESIGN 4

A) Q= 12 L/S

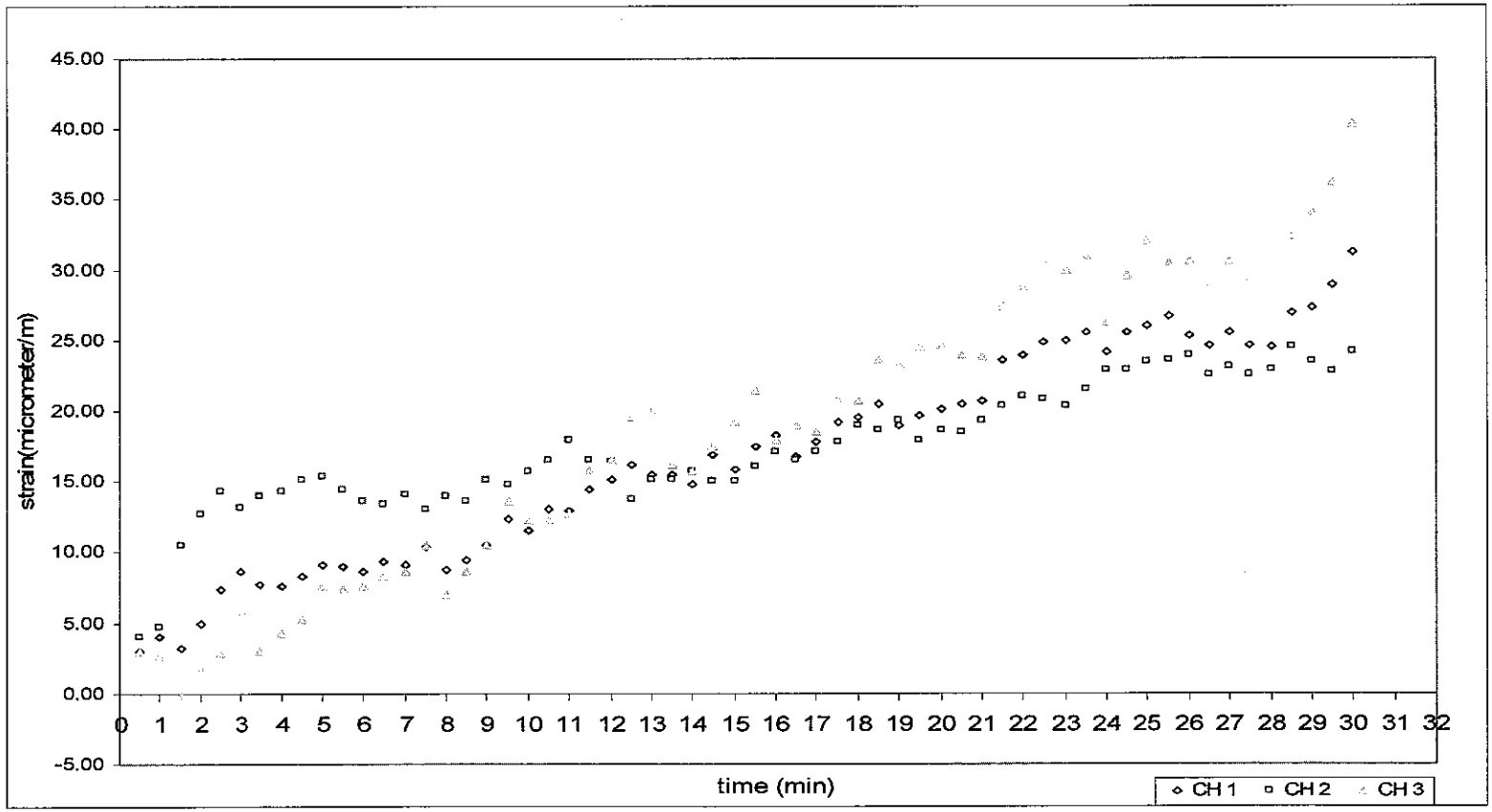

STRAIN- TIME GRAPH

DESIGN 4

B) Q= 30 L/S

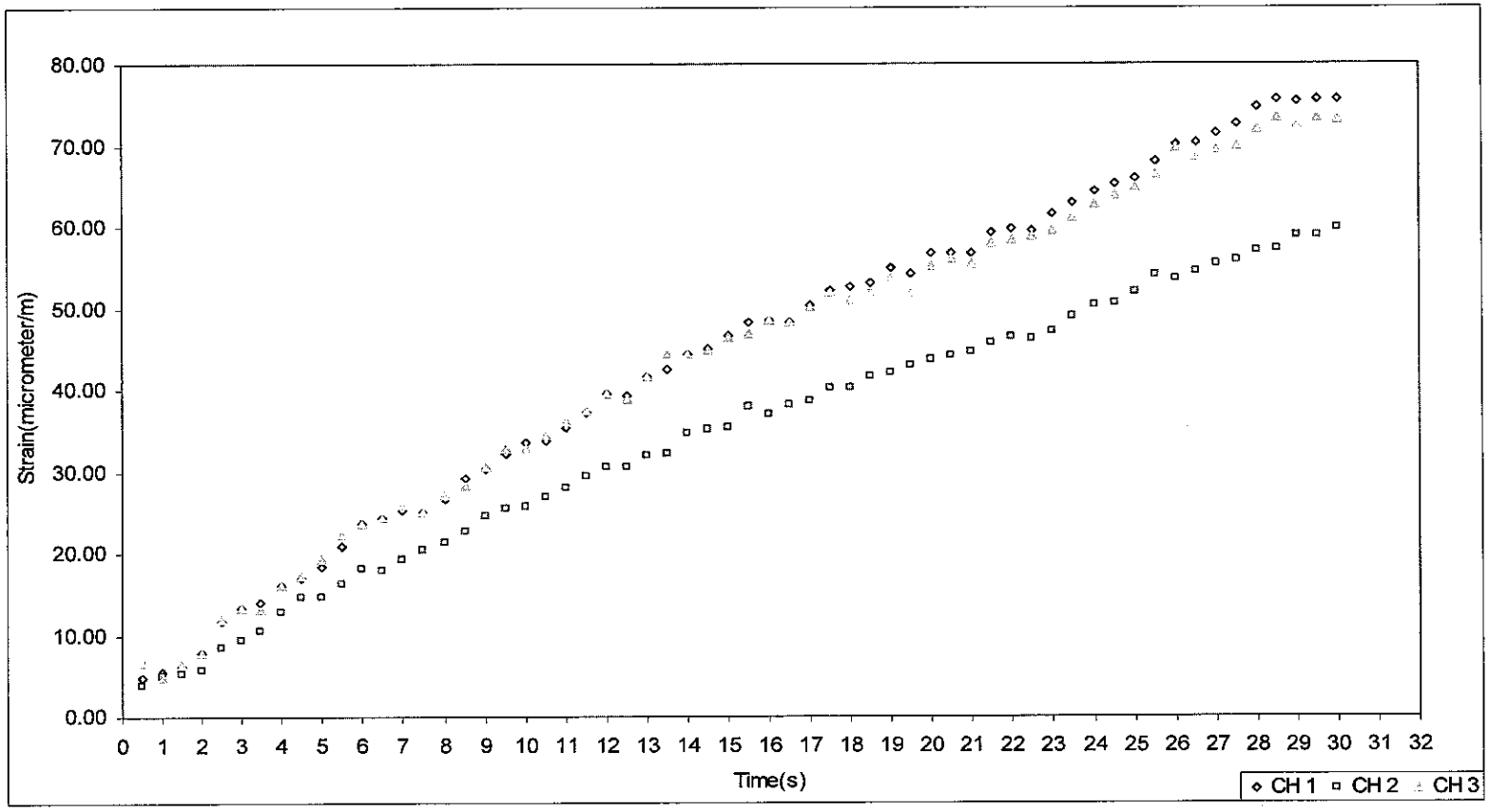

APPENDIX D

CALIBRATION GRAPH

DESIGN 1

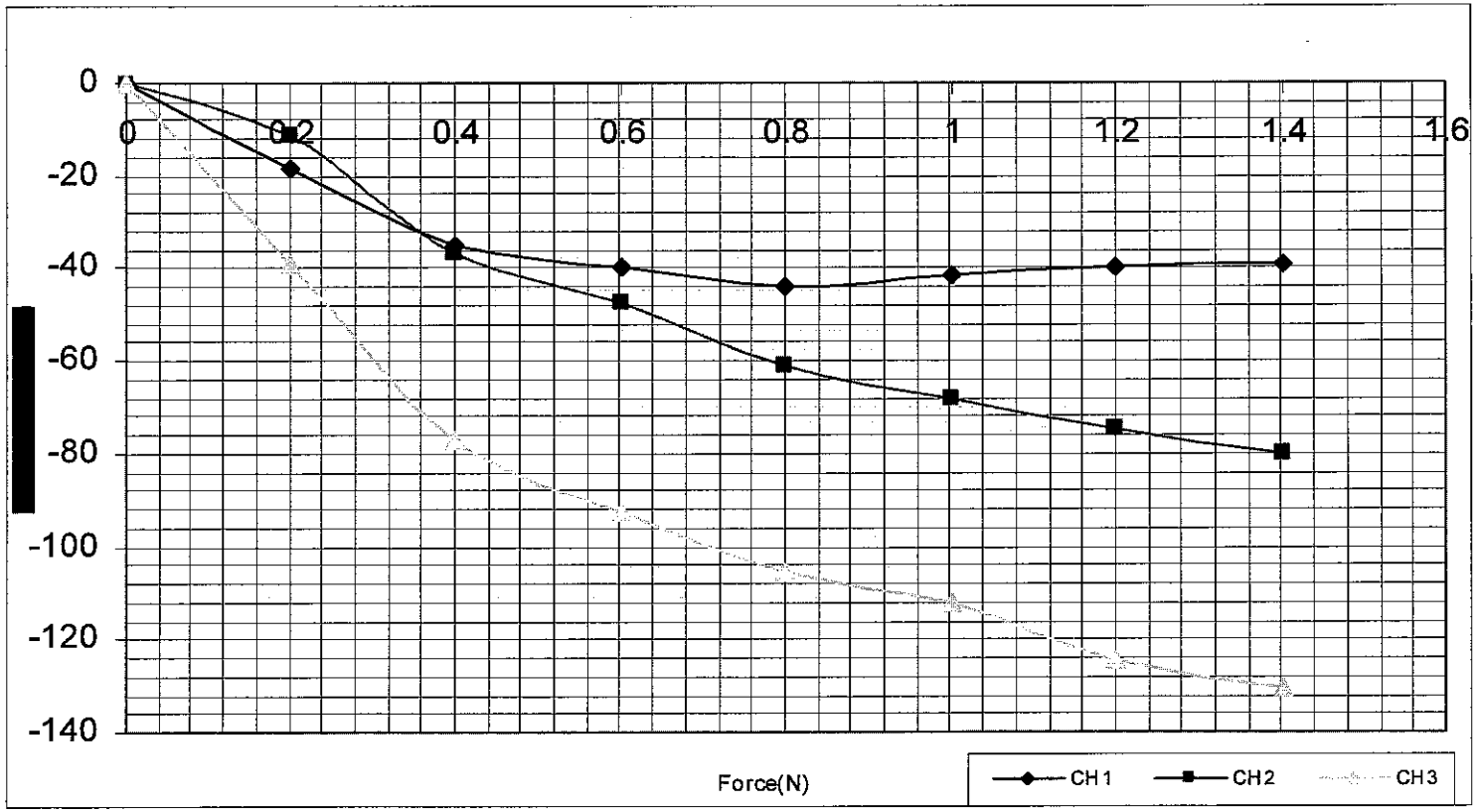

CALIBRATION GRAPH

DESIGN 2

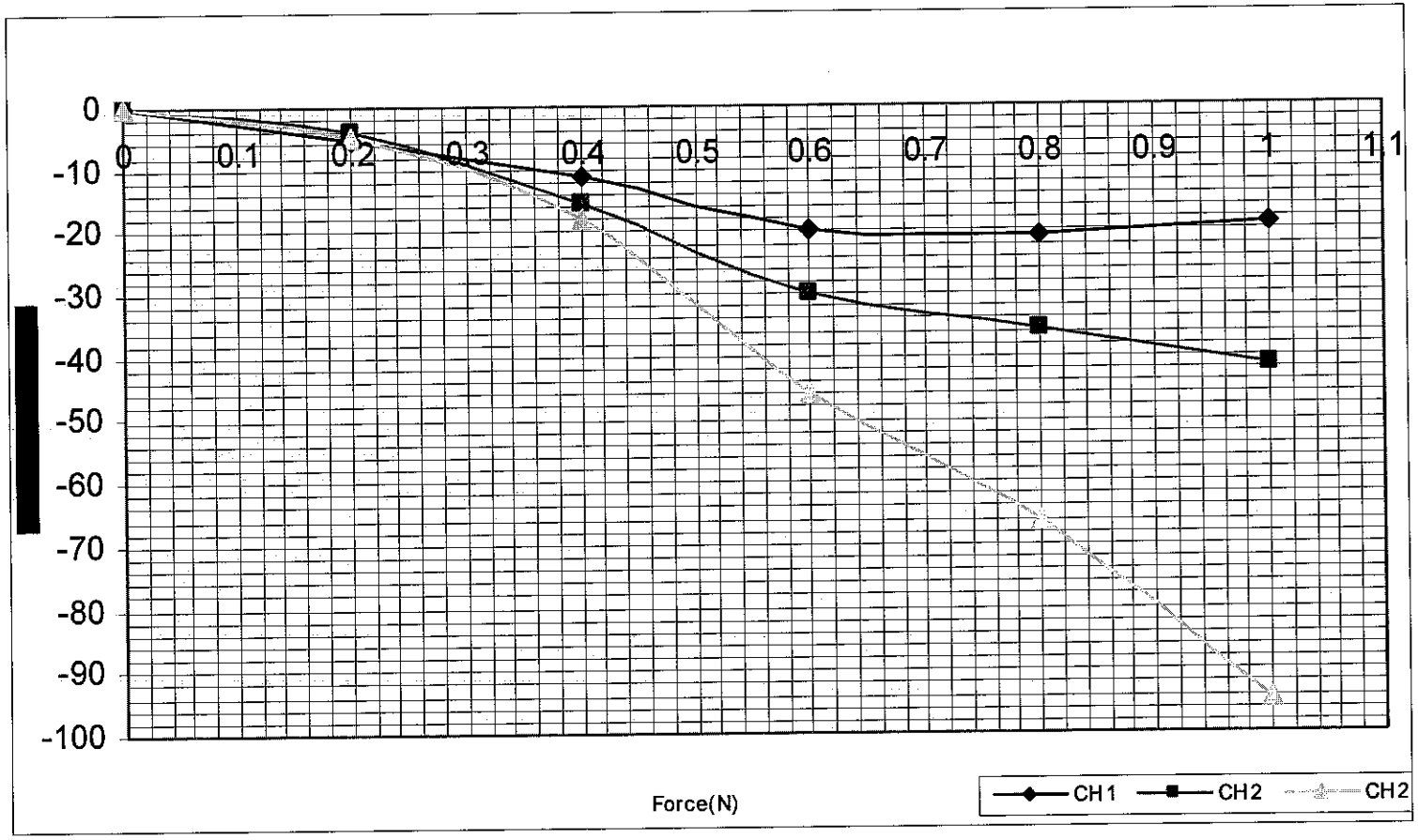

CALIBRATION GRAPH

DESIGN 3

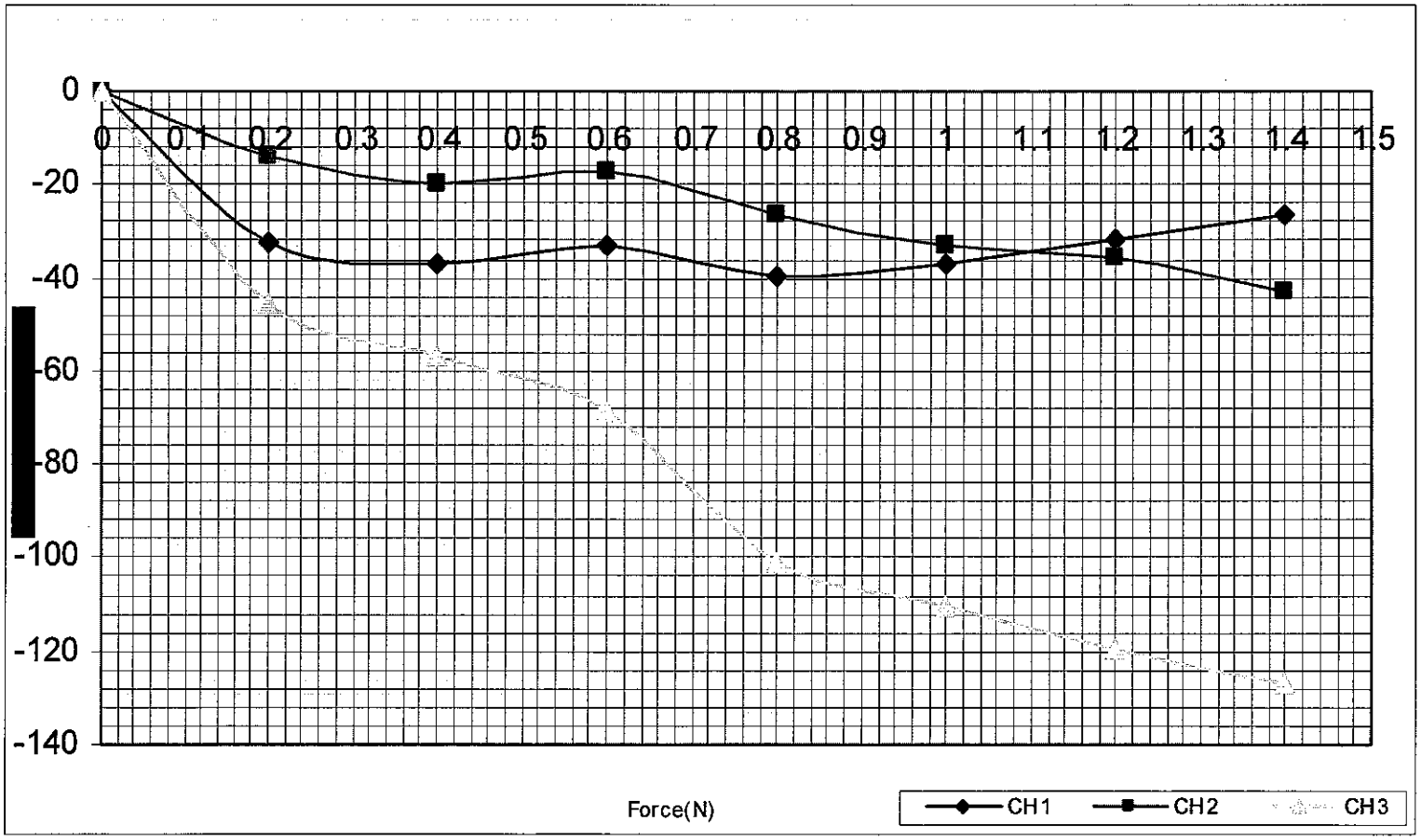

CALIBRATION GRAPH

DESIGN 4

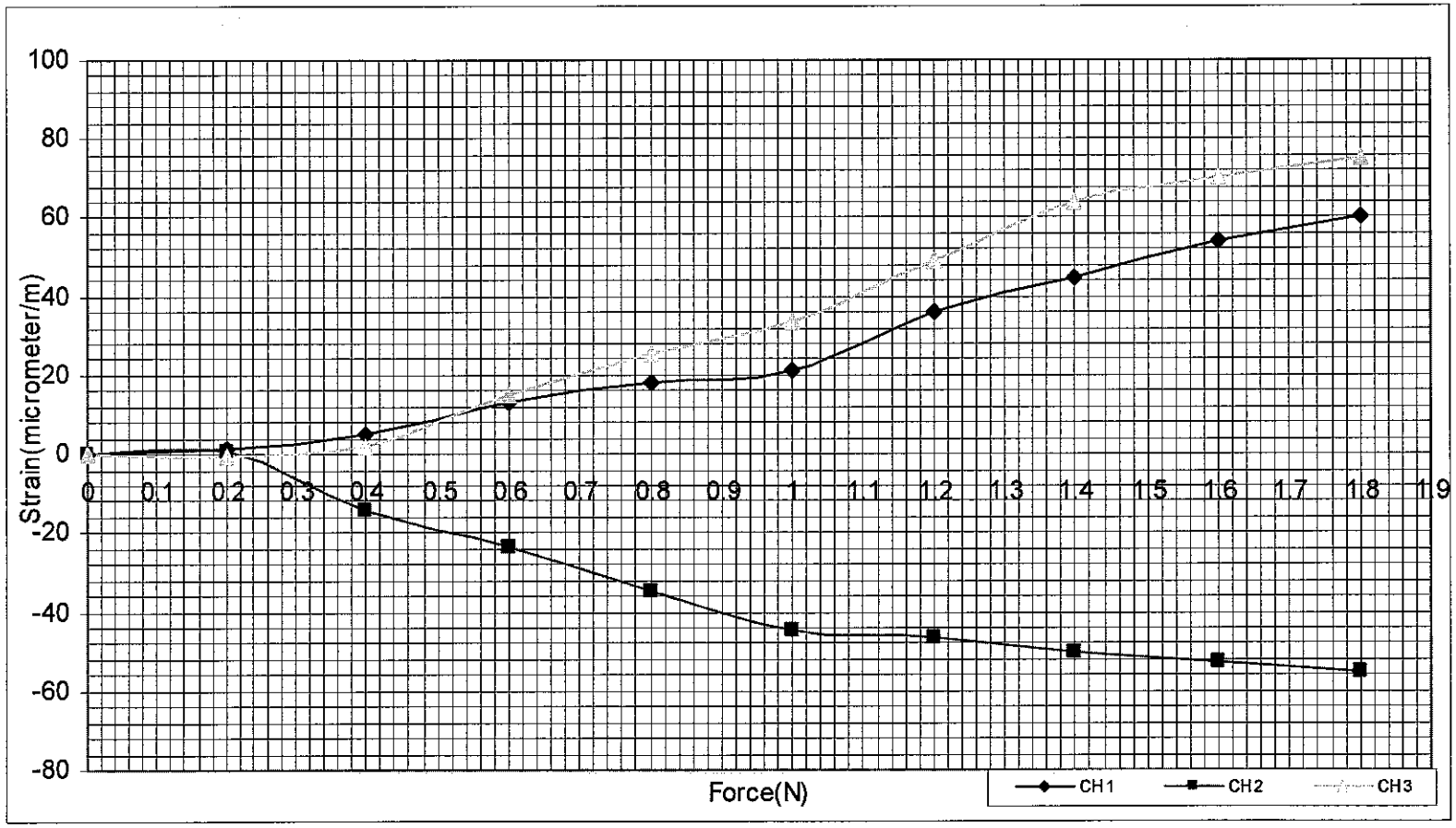

APPENDIX E

EFFECT OF FORCE ON BLOCK SIZE COMPARISON

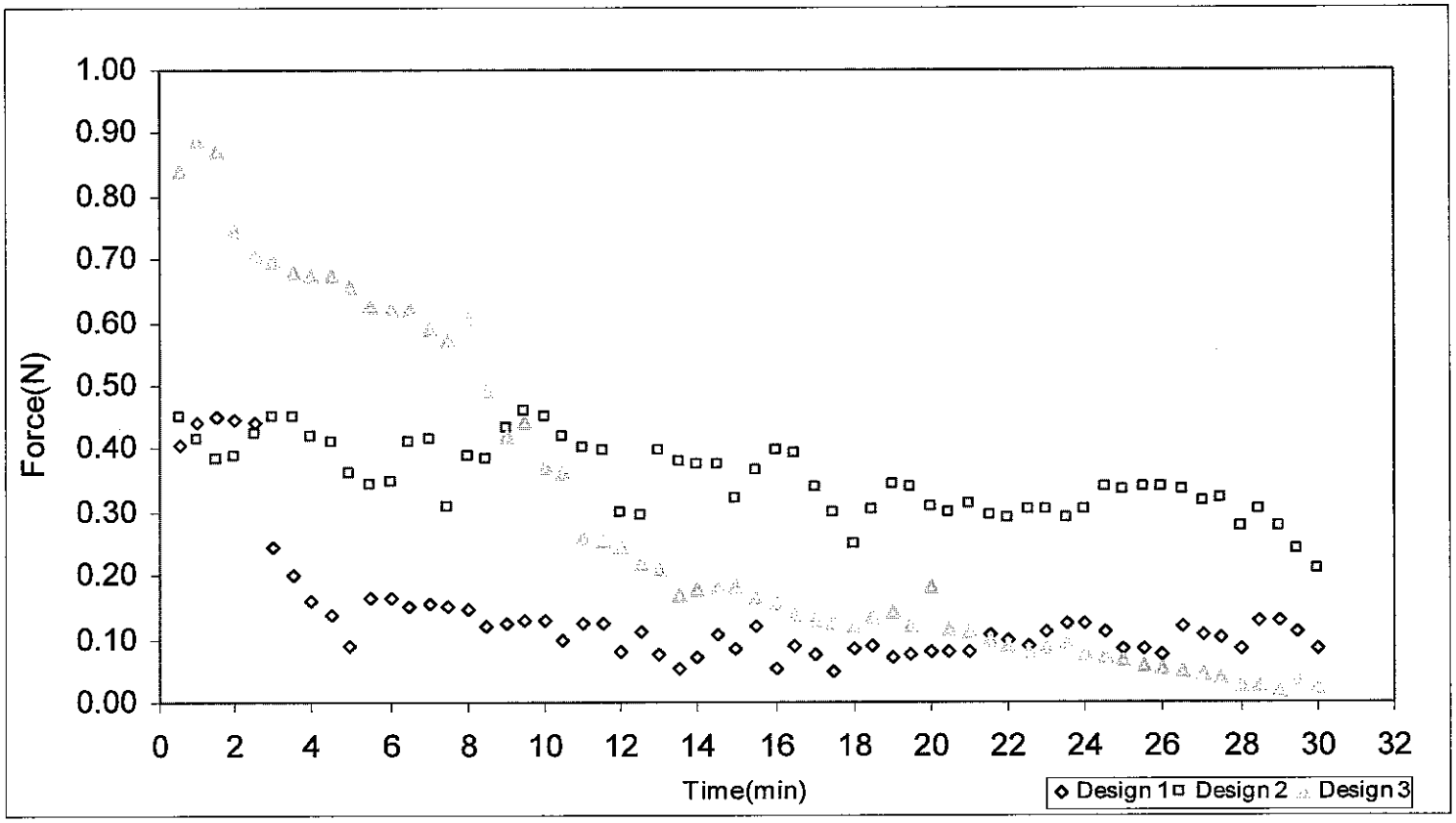

APPENDIX F

GRAPH OF FORCE-TIME

DESIGN 1

A) Q=12 L/S

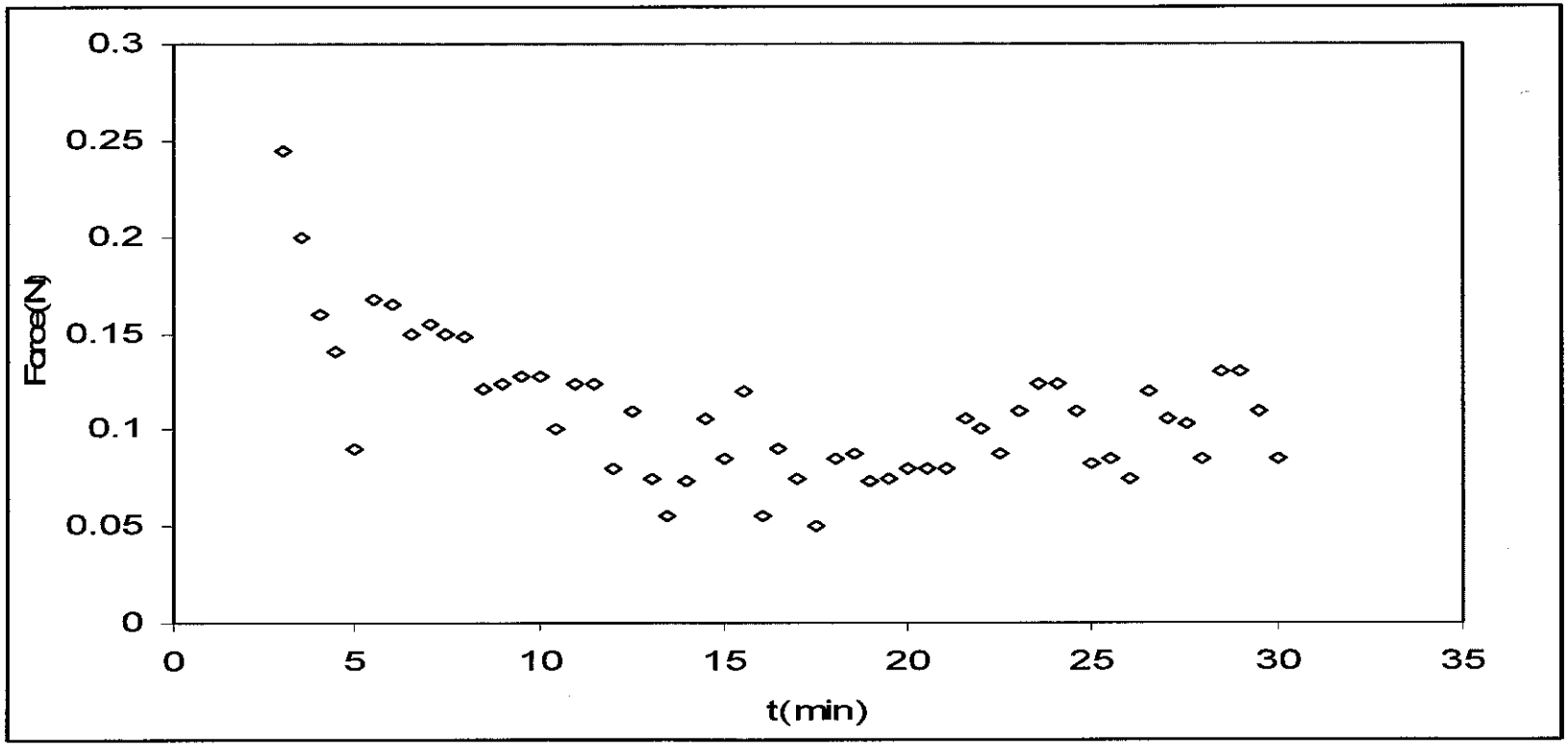

GRAPH OF FORCE-TIME

DESIGN 1

B) Q=30 L/S

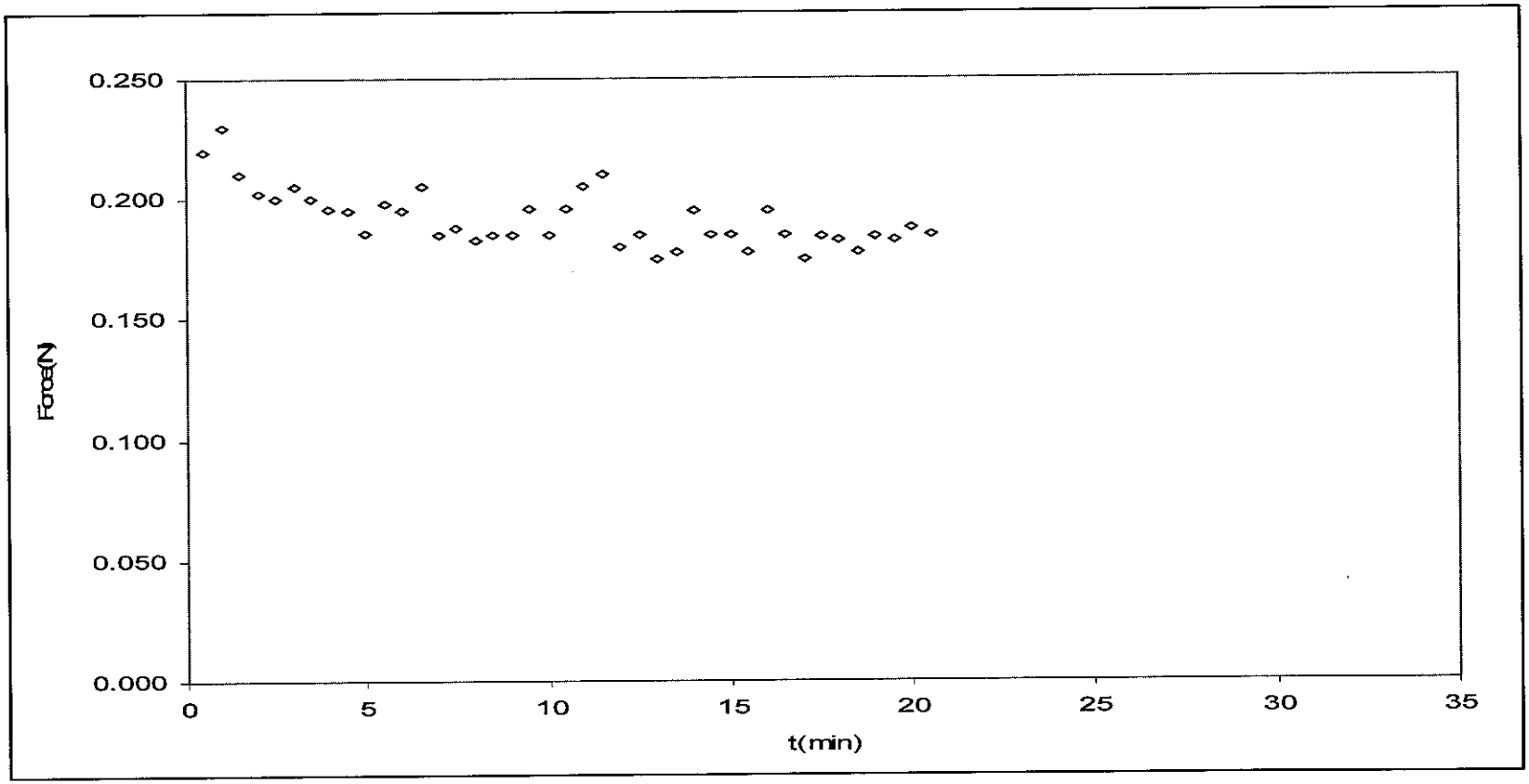

GRAPH OF FORCE-TIME

DESIGN 2

A) Q=12 L/S

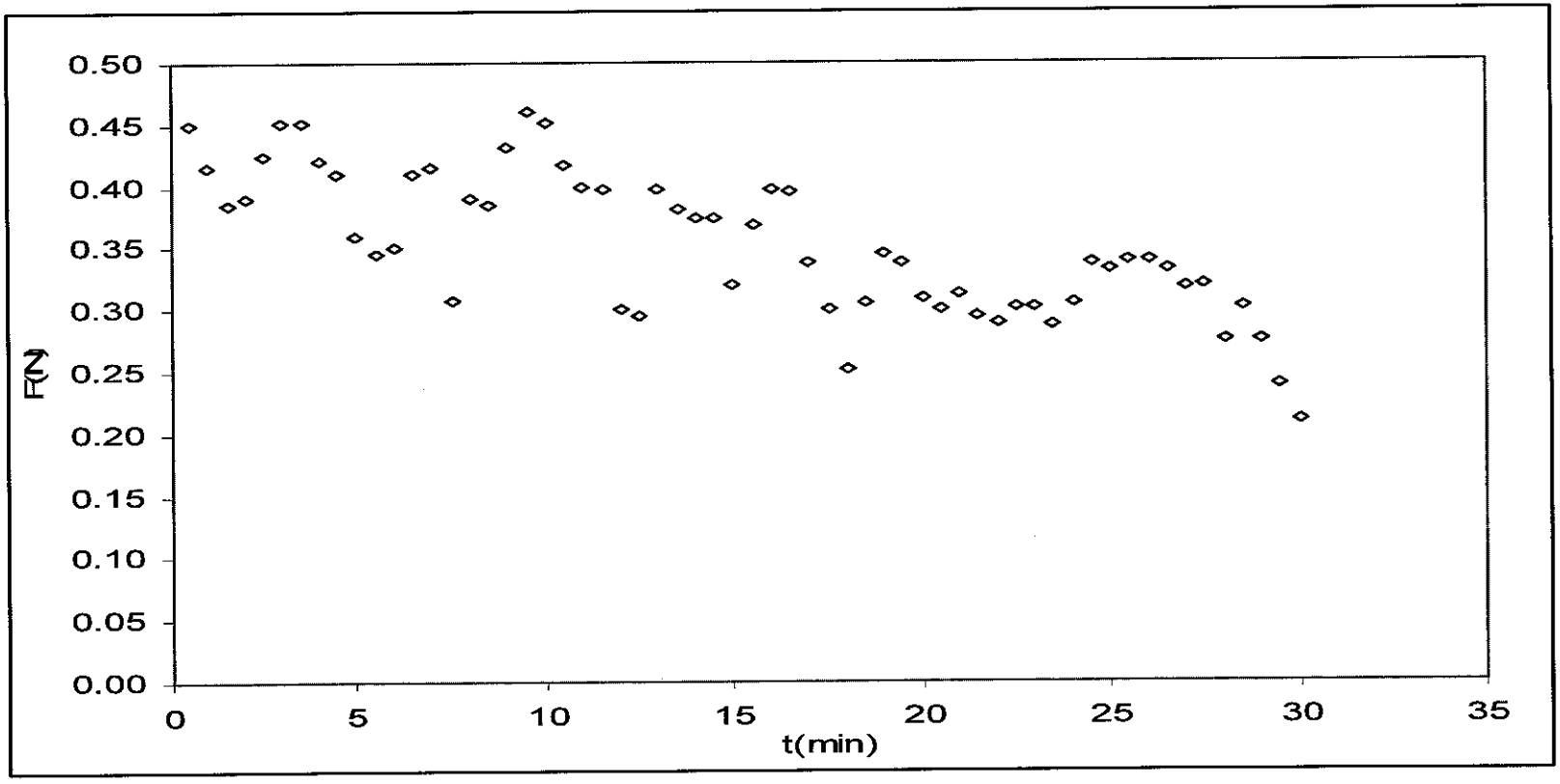

GRAPH OF FORCE-TIME

DESIGN 2

B) Q=30 L/S

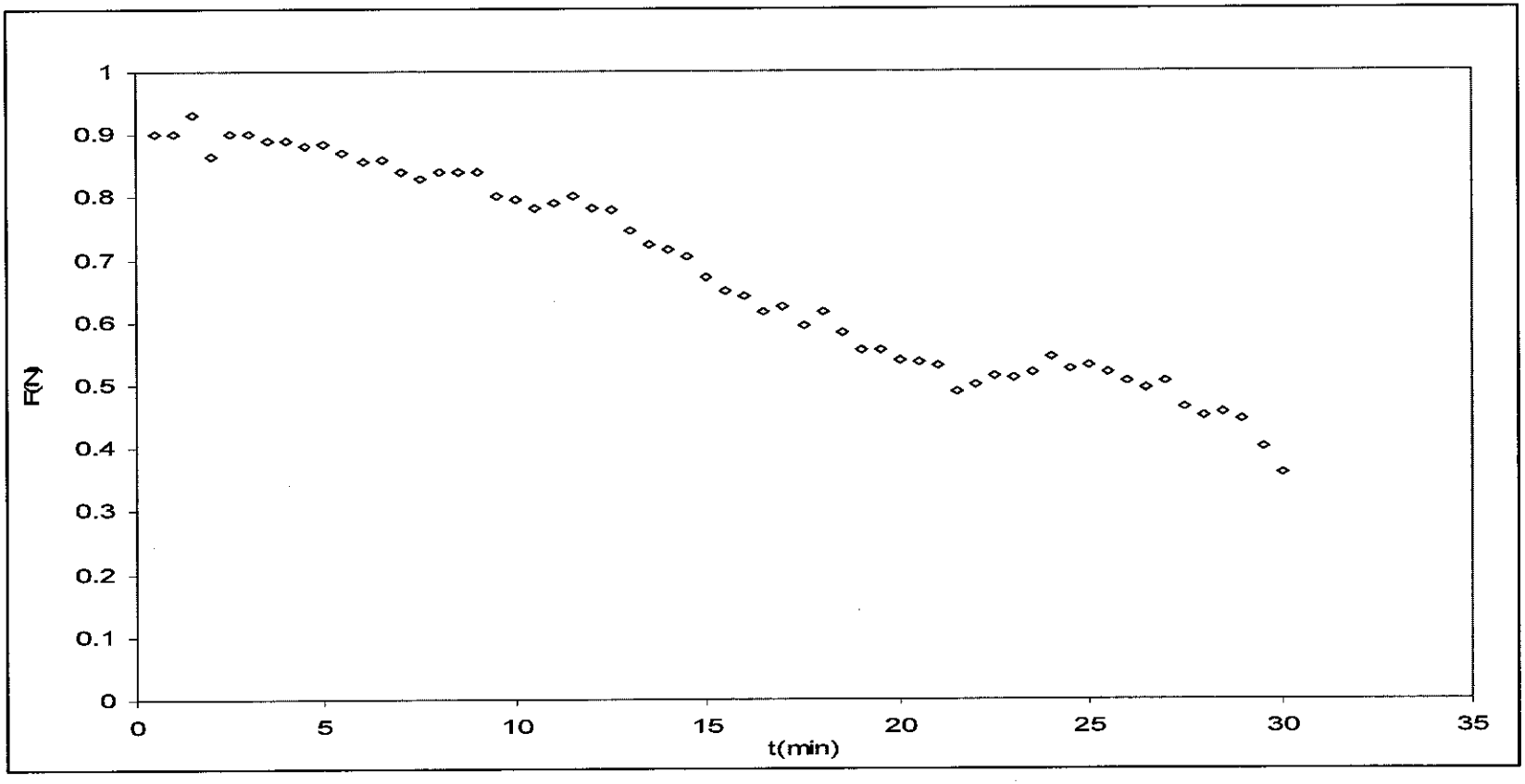

GRAPH OF FORCE-TIME

DESIGN 3

A) Q=12 L/S

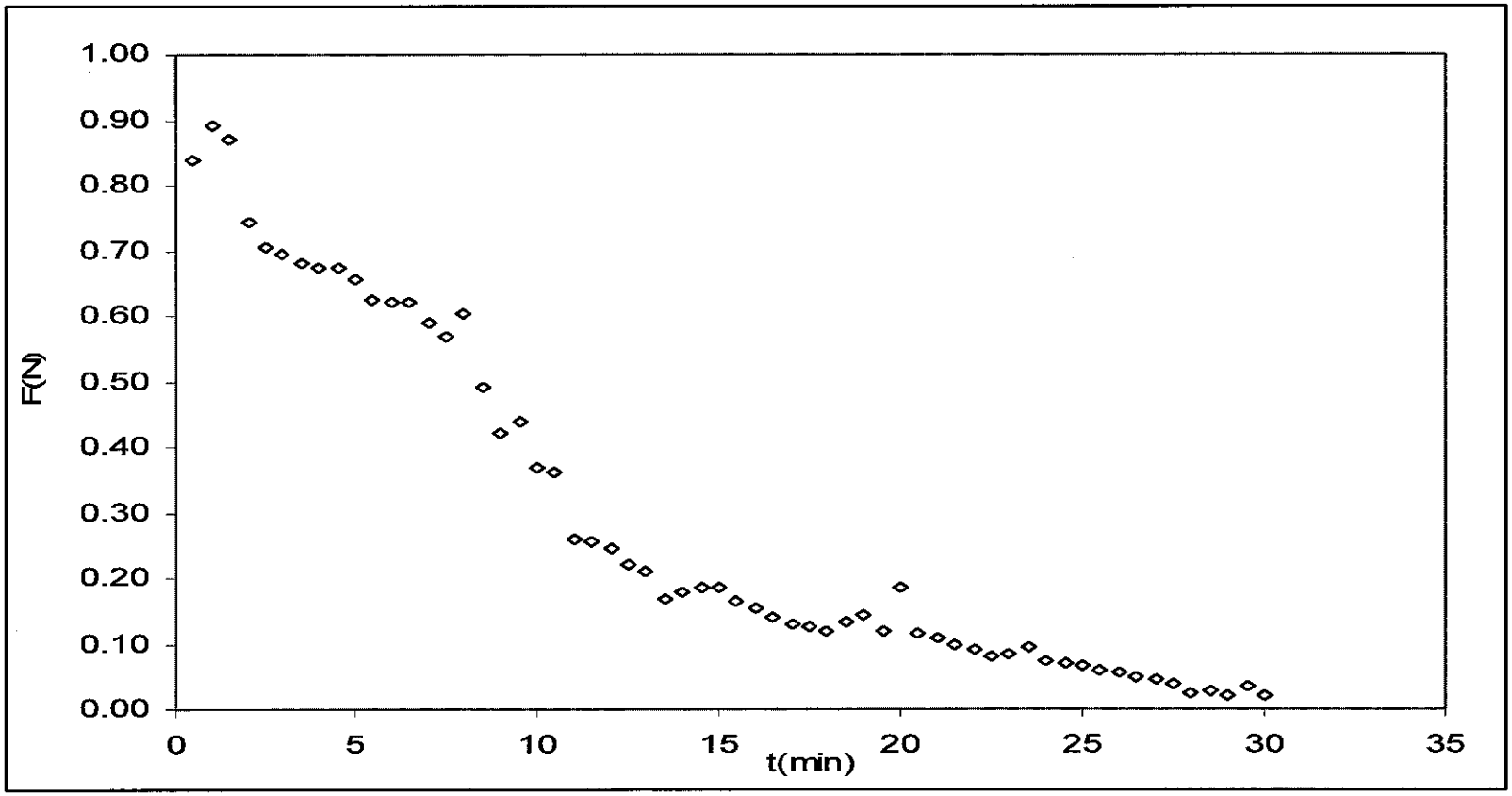

GRAPH OF FORCE-TIME

DESIGN 3

B) Q=30 L/S

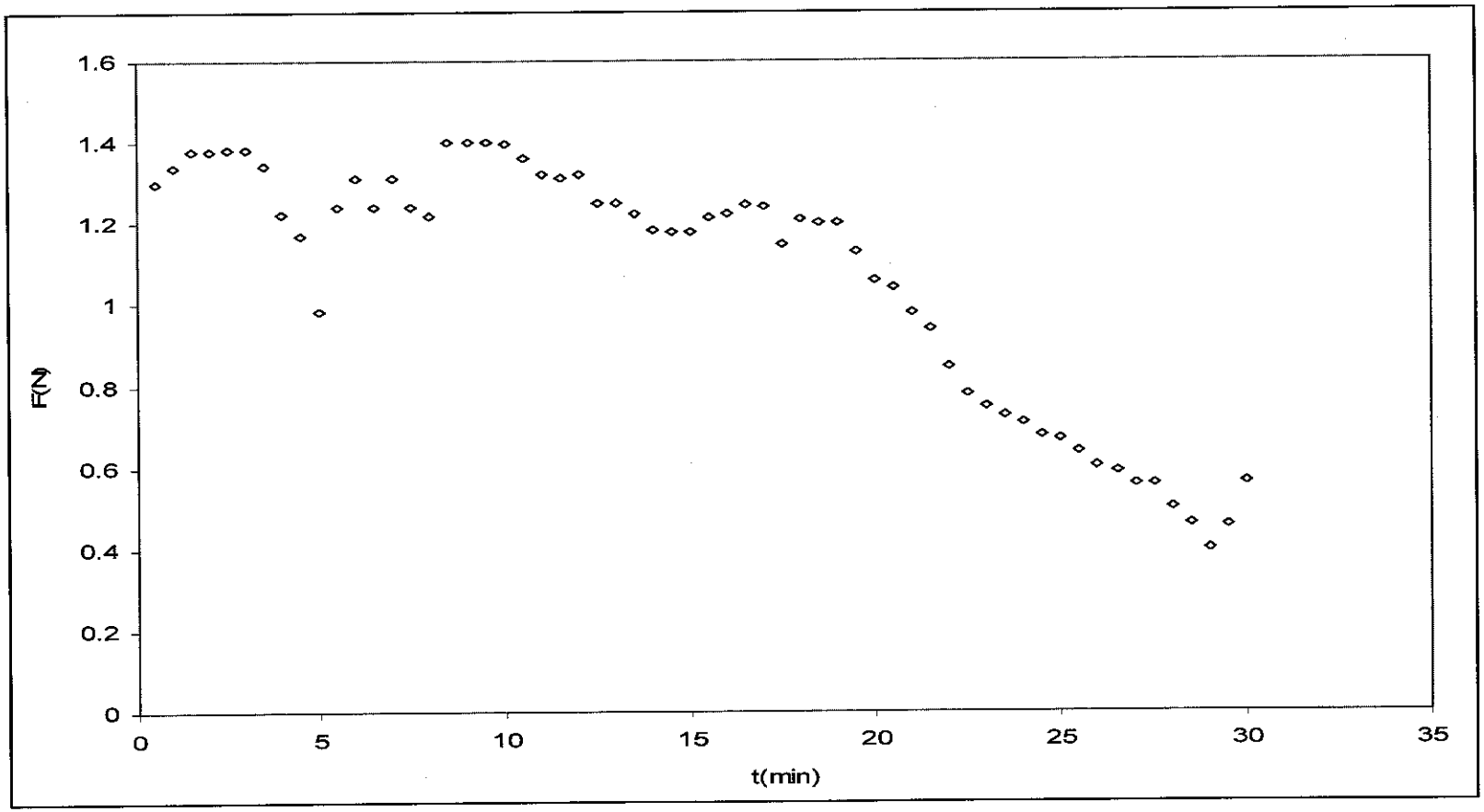

GRAPH OF FORCE-TIME

DESIGN 4

A) Q=12 L/S

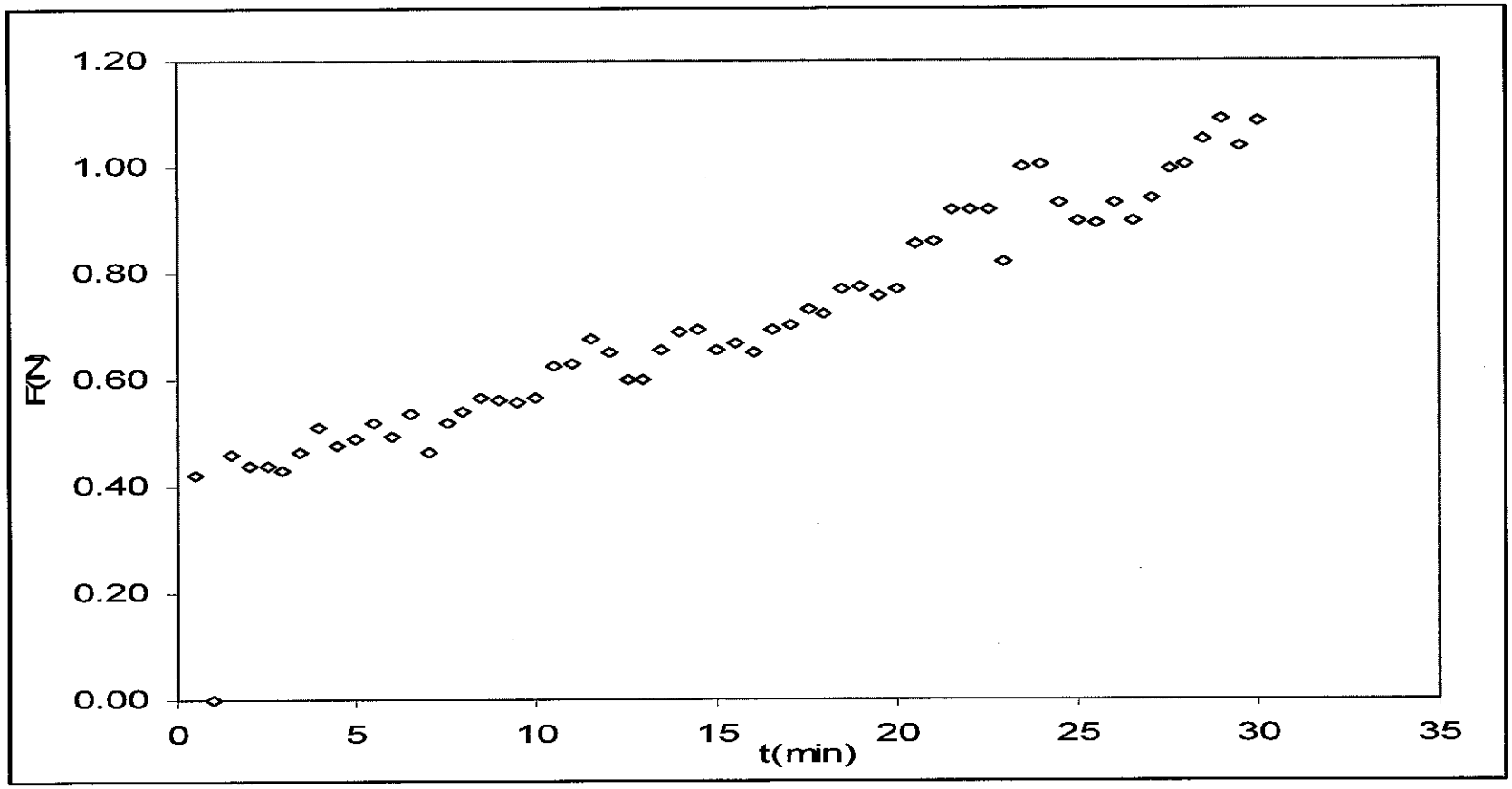

GRAPH OF FORCE-TIME

DESIGN 4

B) Q=30 L/S

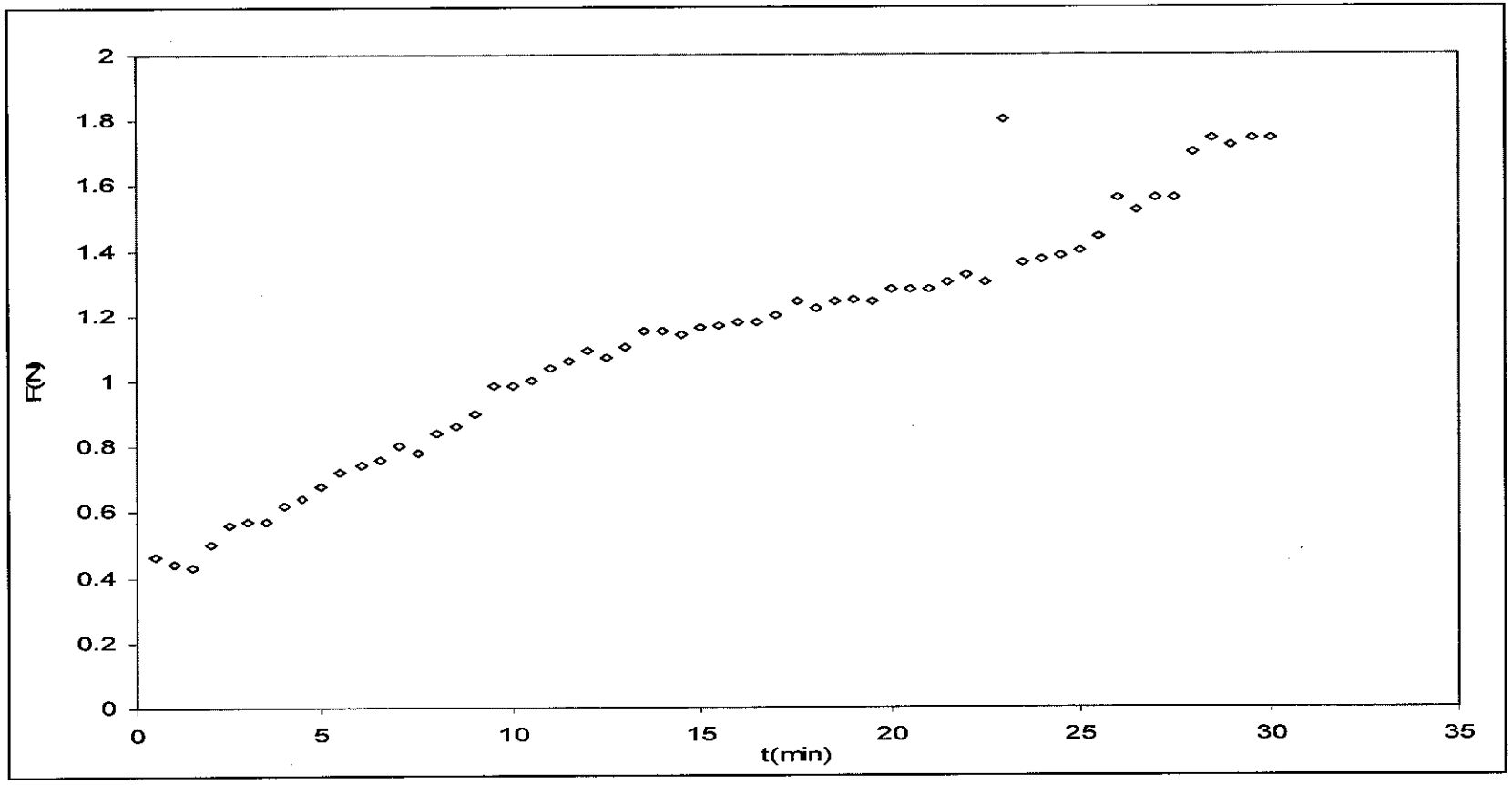

APPENDIX G

DEPTH AND VELOCITY MEASUREMENT DATA

DESIGN 1

Q=12L/S

Point #	T1 (min)	D1 (cm)	V1 (m/s)	T2 (min)	D2 (cm)	V2 (m/s)	T3 (min)	D3 (cm)	V3 (m/s)	T4 (min)	D4 (cm)	V4 (m/s)	T5 (min)	D5 (cm)	V5 (m/s)	T6 (min)	D6 (cm)	V6 (m/s)
1	1.48	8	0.40	8.60	8	0.42	13.98	8	0.39	18.85	8	0.39	24.76	8	0.40	30.22	8	0.41
2	2.48	8	0.29	9.24	8	0.30	14.69	8	0.30	19.61	8	0.26	25.36	8	0.29	30.49	8	0.27
3	3.76	8	0.01	9.90	8	0.02	15.17	8	0.02	20.44	8	0.01	25.97	8	0.01	31.23	8	0.01
4	4.49	8	0.04	10.63	8	0.03	16.28	8	0.10	21.15	8	0.05	26.65	8	0.03	31.83	8	0.05
5	5.15	8	0.24	11.21	8	0.22	17.47	8	0.30	21.93	8	0.23	27.40	8	0.25	32.52	8	0.19
6	6.36	8	0.34	11.85	8	0.30	18.10	8	0.29	22.57	8	0.27	28.07	8	0.26	33.17	8	0.29
7	7.19	8	0.13	12.52	8	0.06	18.31	8	0.04	23.24	8	0.01	28.81	8	0.01	33.92	8	0.01
8	7.84	8	0.20	13.19	8	0.15	18.58	8	0.20	23.93	8	0.25	29.48	8	0.17	34.47	8	0.23

DEPTH AND VELOCITY MEASUREMENT DATA

DESIGN 1

Q=30L/S

Point #	T1 (min)	D1 (cm)	V1 (m/s)	T2 (min)	D2 (cm)	V2 (m/s)	T3 (min)	D3 (cm)	V3 (m/s)	T4 (min)	D4 (cm)	V4 (m/s)	T5 (min)	D5 (cm)	V5 (m/s)	T6 (min)	D6 (cm)	V6 (m/s)
1	0.66	17	0.76	6.46	17	0.80	11.93	17	0.75	17.07	17	0.79	22.42	17	0.78	27.62	17	0.80
2	1.49	17	0.58	7.13	17	0.59	12.59	17	0.55	17.73	17	0.57	23.05	17	0.60	27.81	17	0.61
3	2.29	17	0.04	7.78	17	0.05	13.72	17	0.04	18.36	17	0.06	23.70	17	0.06	28.47	17	0.03
4	3.02	17	0.11	8.39	17	0.09	13.94	17	0.12	19.05	17	0.17	24.32	17	0.15	29.14	17	0.11
5	3.73	17	0.55	9.04	17	0.60	14.83	17	0.55	19.70	17	0.52	24.97	17	0.47	29.85	17	0.50
6	4.49	17	0.56	9.67	17	0.57	15.06	17	0.60	20.38	17	0.58	25.64	17	0.60	30.48	17	0.57
7	5.07	17	0.20	10.36	17	0.22	15.75	17	0.23	21.06	17	0.23	26.26	17	0.25	31.14	17	0.21
8	5.78	17	0.23	11.06	17	0.25	16.39	17	0.27	21.73	17	0.22	26.93	17	0.24	31.82	17	0.21

DEPTH AND VELOCITY MEASUREMENT DATA

DESIGN 2

Q=12L/S

Point #	T1 (min)	D1 (cm)	V1 (m/s)	T2 (min)	D2 (cm)	V2 (m/s)	T3 (min)	D3 (cm)	V3 (m/s)	T4 (min)	D4 (cm)	V4 (m/s)	T5 (min)	D5 (cm)	V5 (m/s)	T6 (min)	D6 (cm)	V6 (m/s)
1	0.71	8	0.41	7.58	9	0.39	13.62	8	0.42	19.52	8	0.45	25.52	8	0.45	31.00	8	0.42
2	1.48	8	0.24	8.36	8	0.20	14.33	8	0.25	20.20	8	0.28	26.26	8	0.29	31.53	8	0.27
3	2.31	8	0.01	9.12	8	0.01	15.17	8	0.01	20.96	8	0.01	26.97	8	0.01	32.22	8	0.01
4	3.34	8	0.04	9.93	8	0.02	15.98	8	0.01	21.76	8	0.05	27.71	8	0.04	33.01	8	0.03
5	4.32	8	0.21	10.71	8	0.17	16.56	8	0.24	22.63	8	0.23	28.41	8	0.24	33.69	8	0.23
6	5.21	8	0.19	11.43	8	0.23	17.31	8	0.25	23.43	8	0.28	29.11	8	0.27	33.45	8	0.24
7	5.95	8	0.02	12.11	8	0.01	18.04	8	0.01	24.06	8	0.01	29.80	8	0.01	35.02	8	0.01
8	6.86	8	0.12	12.89	8	0.11	18.74	8	0.22	24.81	8	0.24	30.70	8	0.16	35.72	8	0.17

DEPTH AND VELOCITY MEASUREMENT DATA

DESIGN 2

Q=30L/S

Point #	T1 (min)	D1 (cm)	V1 (m/s)	T2 (min)	D2 (cm)	V2 (m/s)	T3 (min)	D3 (cm)	V3 (m/s)	T4 (min)	D4 (cm)	V4 (m/s)	T5 (min)	D5 (cm)	V5 (m/s)	T6 (min)	D6 (cm)	V6 (m/s)
1	0.83	15	0.74	7.59	16	0.73	13.53	16	0.70	18.95	16	0.73	24.78	16	0.70	30.36	16	0.70
2	1.63	15	0.60	8.38	16	0.57	14.29	16	0.53	19.77	16	0.60	25.54	16	0.56	31.20	16	0.54
3	2.63	15	0.02	9.26	16	0.02	15.05	16	0.04	20.50	16	0.04	26.30	16	0.02	31.96	16	0.02
4	3.41	15	0.09	10.03	16	0.21	15.75	16	0.19	21.16	16	0.23	26.97	16	0.18	32.63	16	0.27
5	4.23	15	0.42	10.69	16	0.40	15.84	16	0.34	21.84	16	0.43	27.71	16	0.42	33.32	16	0.41
6	5.19	15	0.52	11.37	16	0.51	16.55	16	0.52	22.53	16	0.51	28.29	16	0.51	33.99	16	0.53
7	5.83	15	0.08	12.03	16	0.08	17.34	16	0.05	23.36	16	0.06	29.05	16	0.04	34.54	16	0.03
8	6.61	15	0.24	12.76	16	0.27	18.17	16	0.26	23.98	16	0.24	29.84	16	0.22	35.28	16	0.23

DEPTH AND VELOCITY MEASUREMENT DATA

DESIGN 3

Q=12L/S

Point #	T1 (min)	D1 (cm)	V1 (m/s)	T2 (min)	D2 (cm)	V2 (m/s)	T3 (min)	D3 (cm)	V3 (m/s)	T4 (min)	D4 (cm)	V4 (m/s)	T5 (min)	D5 (cm)	V5 (m/s)	T6 (min)	D6 (cm)	V6 (m/s)
1	0.75	8	0.42	7.03	8	0.42	13.14	8	0.44	18.71	8	0.41	24.34	8	0.41	29.89	8	0.42
2	1.69	7	0.25	7.73	7	0.24	14.02	7	0.23	19.46	7	0.30	25.10	7	0.25	30.51	7	0.25
3	2.59	7	0.02	8.45	7	0.04	14.62	7	0.01	20.21	7	0.01	25.87	7	0.02	31.18	7	0.01
4	3.49	7	0.14	9.16	7	0.15	15.35	7	0.17	20.90	7	0.10	26.64	7	0.15	31.89	7	0.15
5	4.30	7	0.15	9.99	7	0.13	15.90	7	0.12	21.59	7	0.15	27.39	7	0.12	32.60	7	0.12
6	5.01	7	0.13	10.62	7	0.10	16.55	7	0.15	22.25	7	0.16	28.02	7	0.17	33.27	7	0.09
7	5.71	7	0.04	11.39	7	0.03	17.19	7	0.05	22.96	7	0.04	28.77	7	0.03	33.94	7	0.04
8	6.35	7	0.08	12.44	7	0.12	17.89	7	0.12	23.60	7	0.08	29.43	7	0.08	34.62	7	0.06

DEPTH AND VELOCITY MEASUREMENT DATA

DESIGN 3

Q=30L/S

Point #	T1 (min)	D1 (cm)	V1 (m/s)	T2 (min)	D2 (cm)	V2 (m/s)	T3 (min)	D3 (cm)	V3 (m/s)	T4 (min)	D4 (cm)	V4 (m/s)	T5 (min)	D5 (cm)	V5 (m/s)	T6 (min)	D6 (cm)	V6 (m/s)
1	0.77	15	0.80	6.57	15	0.78	12.00	15	0.81	18.35	15	0.79	24.63	15	0.79	30.33	15	0.81
2	1.63	15	0.62	7.25	15	0.57	12.98	15	0.60	19.20	15	0.56	25.34	15	0.61	30.94	15	0.57
3	2.33	15	0.07	7.95	15	0.08	13.80	15	0.05	19.89	15	0.02	26.03	15	0.05	31.63	15	0.05
4	3.07	15	0.05	8.64	15	0.09	14.64	15	0.08	20.83	15	0.18	26.88	15	0.15	32.38	15	0.20
5	3.83	15	0.35	9.30	15	0.43	15.16	15	0.35	21.56	15	0.37	27.61	15	0.34	33.08	15	0.31
6	4.41	15	0.49	9.92	15	0.42	16.11	15	0.46	22.27	15	0.43	28.30	15	0.48	33.74	15	0.45
7	5.15	15	0.12	10.62	15	0.15	16.90	15	0.13	23.07	15	0.12	29.08	15	0.13	34.50	15	0.12
8	5.79	15	0.17	11.27	15	0.19	17.53	15	0.14	23.79	15	0.18	29.78	15	0.20	35.03	15	0.19

DEPTH AND VELOCITY MEASUREMENT DATA

DESIGN 4

Q=12L/S

Point #	T1 (min)	D1 (cm)	V1 (m/s)	T2 (min)	D2 (cm)	V2 (m/s)	T3 (min)	D3 (cm)	V3 (m/s)	T4 (min)	D4 (cm)	V4 (m/s)	T5 (min)	D5 (cm)	V5 (m/s)	T6 (min)	D6 (cm)	V6 (m/s)
1	0.66	8	0.49	7.64	8	0.44	13.83	8	0.41	20.72	8	0.40	26.28	8	0.40	31.96	8	0.40
2	1.43	7	0.26	8.45	8	0.21	14.71	8	0.23	21.42	8	0.23	27.10	8	0.21	32.96	8	0.20
3	2.94	7	0.03	9.17	8	0.01	15.67	8	0.10	22.08	8	0.01	27.87	8	0.01	33.23	8	0.03
4	3.85	7	0.17	9.86	8	0.12	16.84	8	0.16	22.74	8	0.13	28.62	8	0.14	33.97	8	0.05
5	4.68	8	0.19	10.53	8	0.16	17.55	8	0.12	23.39	8	0.16	29.36	8	0.14	34.67	8	0.10
6	5.46	8	0.06	11.23	8	0.06	18.27	8	0.08	24.18	8	0.08	29.97	8	0.07	35.30	8	0.08
7	6.17	8	0.19	12.15	8	0.08	18.96	8	0.08	24.66	8	0.07	30.65	8	0.15	35.97	8	0.05
8	6.87	8	0.05	13.07	8	0.05	19.71	8	0.02	25.39	8	0.02	31.44	8	0.03	36.65	8	0.05

DEPTH AND VELOCITY MEASUREMENT DATA

DESIGN 4

Q=30L/S

Point #	T1 (min)	D1 (cm)	V1 (m/s)	T2 (min)	D2 (cm)	V2 (m/s)	T3 (min)	D3 (cm)	V3 (m/s)	T4 (min)	D4 (cm)	V4 (m/s)	T5 (min)	D5 (cm)	V5 (m/s)	T6 (min)	D6 (cm)	V6 (m/s)
1	1.12	15	0.82	7.67	15	0.81	14.74	15	0.80	22.56	15	0.83	28.84	15	0.85	34.75	15	0.81
2	2.12	15	0.75	8.27	15	0.64	15.49	15	0.40	23.81	15	0.64	29.69	15	0.55	35.41	15	0.58
3	2.90	15	0.12	9.07	15	0.07	16.30	15	0.10	24.53	15	0.14	30.43	15	0.15	36.12	15	0.06
4	3.66	15	0.22	9.71	15	0.31	17.33	15	0.21	25.17	15	0.20	31.18	15	0.24	37.01	15	0.22
5	4.52	15	0.44	10.49	15	0.52	17.91	15	0.51	25.88	15	0.66	31.86	15	0.48	37.70	15	0.38
6	5.28	15	0.42	11.21	15	0.42	18.62	15	0.43	26.53	15	0.38	32.57	15	0.50	38.34	15	0.40
7	5.92	15	0.17	12.03	15	0.19	19.49	15	0.17	27.21	15	0.20	33.29	15	0.15	38.98	15	0.14
8	6.69	15	0.21	12.61	15	0.25	20.64	15	0.23	27.93	15	0.27	34.25	15	0.20	39.69	15	0.24

APPENDIX H

PICTURES OF EXPERIMENTAL WORK IN PERGAU POND

Data Logger set- up work

Depth and Velocity measurement

Orifice Meter installation by technicians

Baffle block model soaked in water for calibration activity

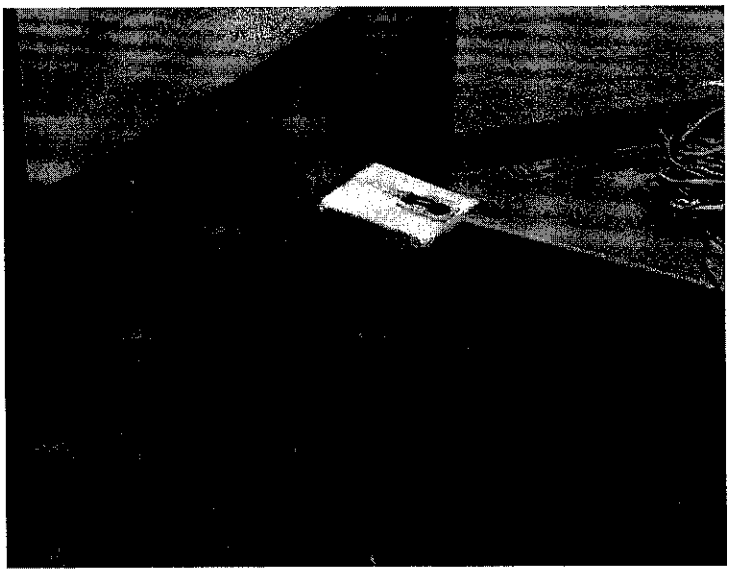

Soft block model pasted on the wall for calibration activity

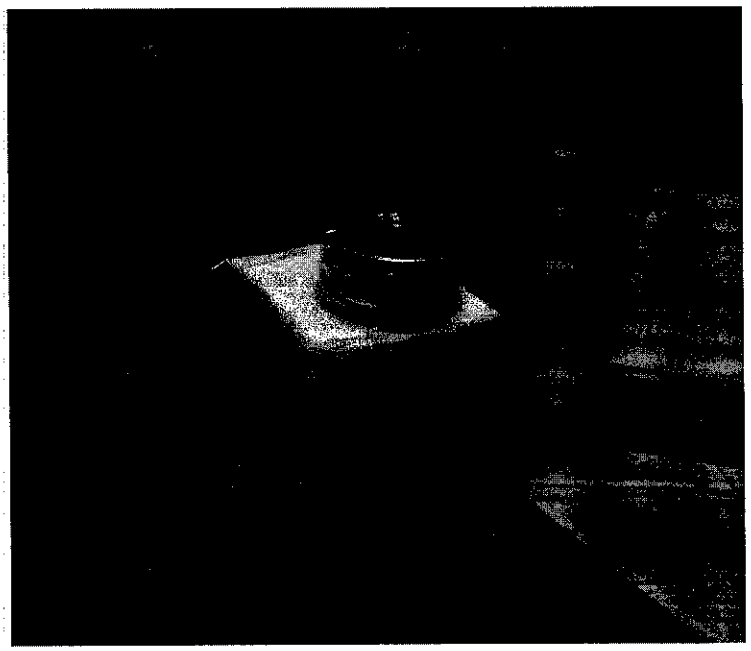

Calibration activity

PICTURES OF PERGAU POND MODEL STRUCTURES

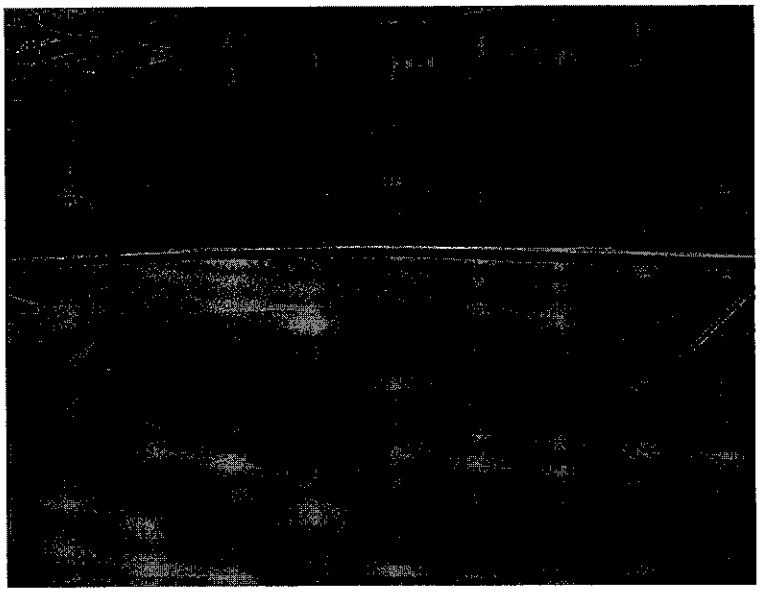

Overview of Pergau Pond Model

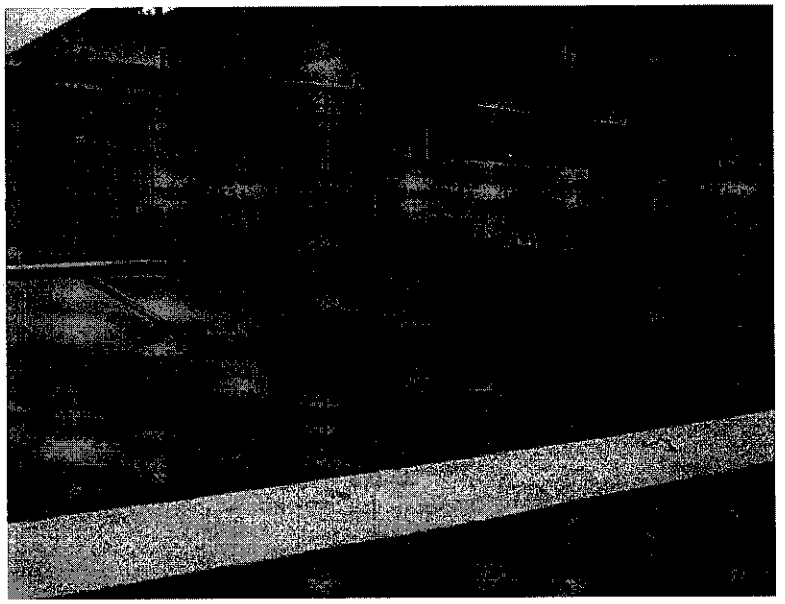

Overview of Pergau Pond Model

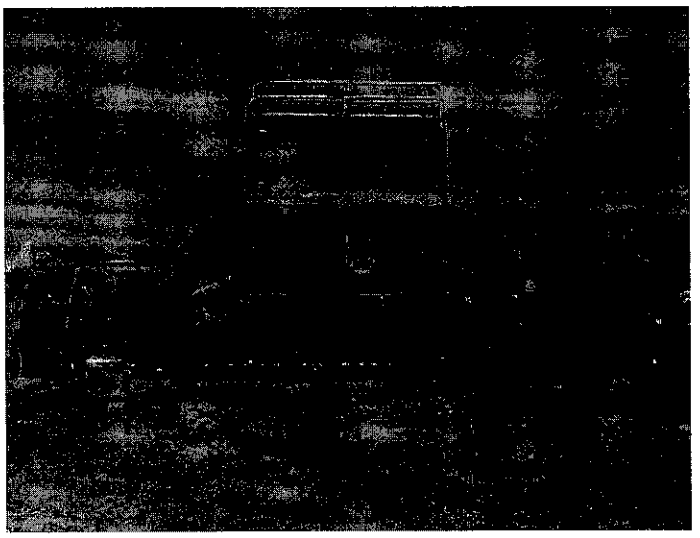

Outlet Structure of Pergau pond model

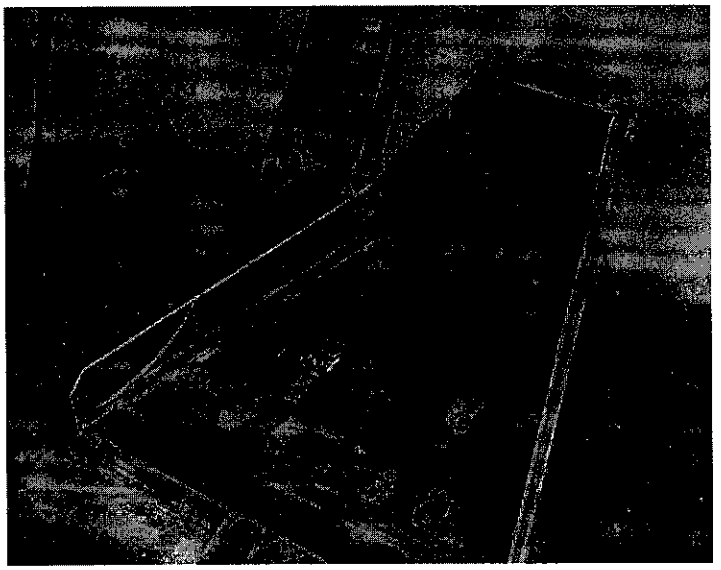

Tailrace Outfall Structure(TOS)

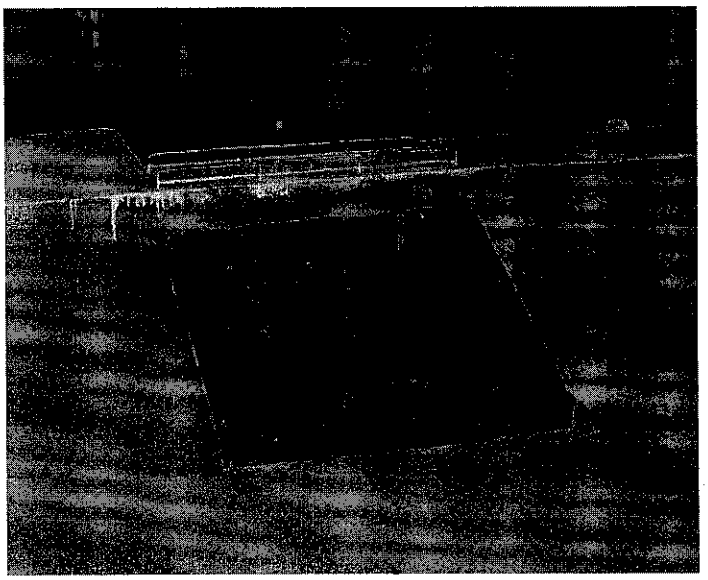

Siphon Spillway of the model

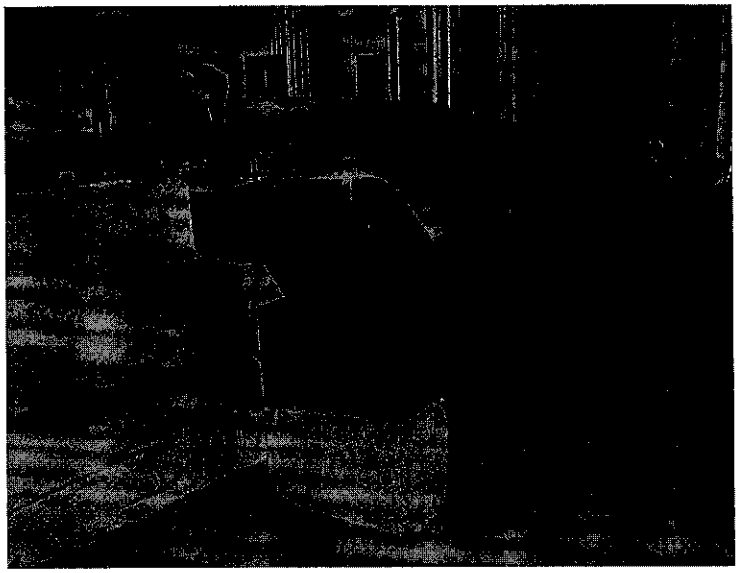

Outlet Drain